Icarus 223 (2013) 11–27

Contents lists available at SciVerse ScienceDirect

Icarus

journal homepage: www.elsevier.com/locate/icarus

A sensitive search for organics (CH_4, CH_3OH, H_2CO, C_2H_6, C_2H_2, C_2H_4), hydroperoxyl (HO_2), nitrogen compounds (N_2O, NH_3, HCN) and chlorine species (HCl, CH_3Cl) on Mars using ground-based high-resolution infrared spectroscopy

G.L. Villanueva [a,b,*], M.J. Mumma [a], R.E. Novak [c], Y.L. Radeva [a,b], H.U. Käufl [d], A. Smette [e], A. Tokunaga [f], A. Khayat [f], T. Encrenaz [g], P. Hartogh [h]

[a] Solar System Exploration Division, Mailstop 690, NASA Goddard Space Flight Center, Greenbelt, MD 20771, USA
[b] Department of Physics, Catholic University of America, Washington, DC 20064, USA
[c] Department of Physics, Iona College, New Rochelle, NY 10801, USA
[d] European Southern Observatory (ESO), München, Germany
[e] European Southern Observatory (ESO), Santiago, Chile
[f] Institute for Astronomy, University of Hawaii, Honolulu, HI 96822, USA
[g] Observatoire Paris-Site de Meudon, LEISA, Paris, Meudon 92195, France
[h] Max Planck Institute for Solar System Research, Katlenburg-Lindau 37191, Germany

ARTICLE INFO

Article history:
Received 27 September 2012
Revised 2 November 2012
Accepted 3 November 2012
Available online 21 November 2012

Keywords:
Mars, Atmosphere
Organic chemistry
Astrobiology
Spectroscopy
Infrared observations

ABSTRACT

Is Mars actively releasing organic and other minor gases into the atmosphere? We present a comprehensive search for trace species on Mars, targeting multiple volatile organic species (CH_4, CH_3OH, H_2CO, C_2H_6, C_2H_2, C_2H_4), hydroperoxyl (HO_2), several nitrogen compounds (N_2O, NH_3, HCN), and two chlorine species (HCl, CH_3Cl) through their rovibrational spectra in the 2.8–3.7 μm spectral region. The data were acquired over a period of 4 years (2006–2010) using powerful infrared high-resolution spectrometers (CRIRES, NIRSPEC, CSHELL) at high-altitude observatories (VLT, Keck-2, NASA-IRTF), and span a broad range of seasons, Doppler shifts and spatial coverage. Here, we present results from a selection of high-quality spectra obtained on four separate dates, representing a fraction of our search space. For most of these species we derived the most stringent upper limits ever obtained, and because the targeted gases have substantially different resident lifetimes in the Martian atmosphere (from hours to centuries), our measurements not only test for current release but also provide stringent limits on the quiescent levels. In particular, we sampled the same regions where plumes of methane have been recently observed (e.g., Syrtis Major and Valles Marineris), allowing us to test for seasonal and temporal variability.

1. Introduction

Even though numerous spacecraft have been sent to Mars and geological formations including their mineralogy are known in great detail, relatively little is known of the composition of the martian atmosphere. The atmosphere is primarily composed of CO_2 (95.3%), with modest volatile nitrogen (N_2, 2.7%), oxygen (O_2, 0.13%), hydrogen (e.g., $H_2O \sim 0.02\%$) and various noble gases (Ar, 1.6%, and traces of Ne, Kr and Xe) (Encrenaz et al. (2004b) and refs. therein). Other detected minor species, such as CO, O_3, H_2O_2, and NO are produced photochemically from these primary volatiles (see Fig. 1).

The martian surface shows scars of a rich geological history and even of flowing liquid water (e.g., Carr and Head, 2003). Many indicators suggest that the planet hosted habitable conditions during the Noachian age (3.7–4.5 byr ago), probably leading to the formation of rich subsurface aqueous reservoirs. Subsurface hydrates surviving from that time could incorporate methane produced by geological processes or by living organisms. Measurements of epithermal neutron fluxes obtained by Mars Odyssey (Feldman et al., 2004), suggest the presence of important near-surface hydrogen concentrations on Mars. This hydrogen is often interpreted as buried water ice; however, independent evidence is required to establish its chemical form (e.g., hydrocarbons and/or mineral hydrates) in low-latitude sites. Specifically, a detection of enhanced hydrocarbons at these sites could test whether sub-surface hydrogen is chemically bound in hydrocarbon moieties, and would strengthen the possibility of a habitable environment in the sub-surface of

* Corresponding author at: Solar System Exploration Division, Mailstop 690, NASA Goddard Space Flight Center, Greenbelt, MD 20771, USA.
E-mail address: Geronimo.Villanueva@nasa.gov (G.L. Villanueva).

0019-1035/$ - see front matter © 2012 Elsevier Inc. All rights reserved.
http://dx.doi.org/10.1016/j.icarus.2012.11.013

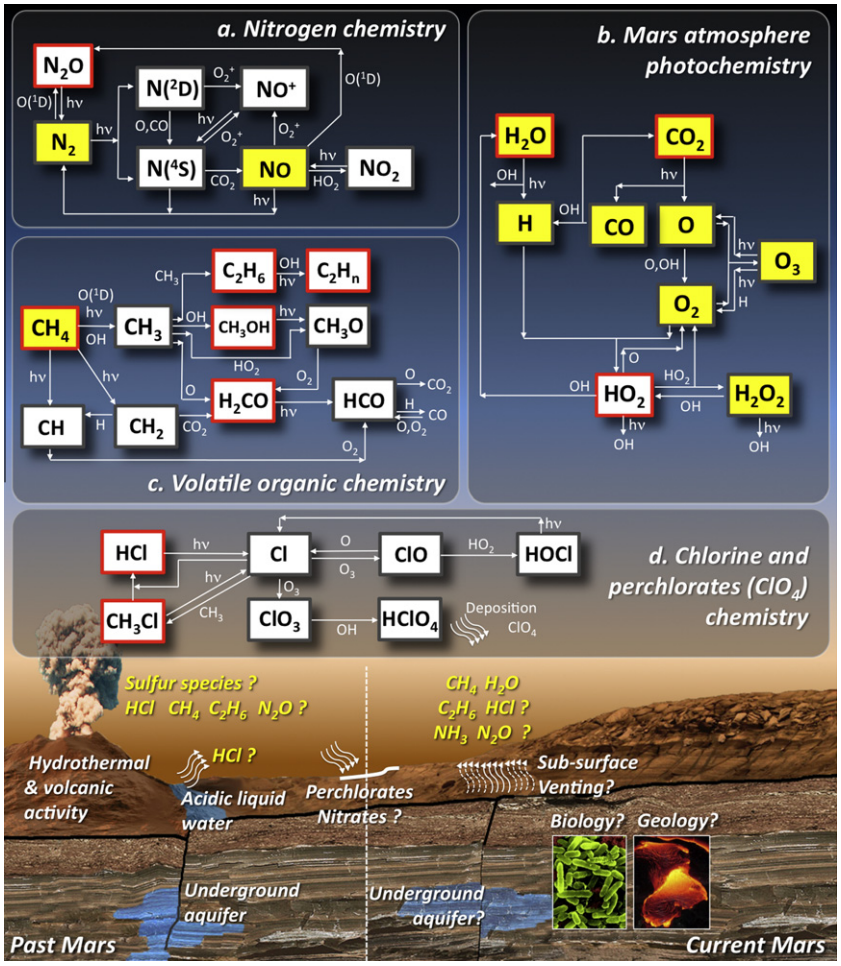

Fig. 1. Possible processes and chemical reactions in the martian atmosphere. In the past, the composition of the atmosphere was probably much richer, ultimately leading to the probable deposition and storage of nitrates and perchlorates into the martian soil. If any geological, hydrothermal or even biological processes are currently active in the martian sub-surface, vents rich in volatile organics and other compounds should be observed. The chemical reaction networks are based on the works of (a) Barth et al. (1992), (b) Atreya et al. (2007), (c) Wong et al. (2004), and (d) Catling et al. (2010). Yellow boxes point to the detected species (Encrenaz et al., 2004b and refs. therein) within each network, while red outlined boxes indicate the molecules searched by this study. (For interpretation of the references to color in this figure legend, the reader is referred to the web version of this article.)

Mars. For this reason, the search for methane (CH_4), its oxidation products (H_2CO, CH_3OH), and other biomarker gases on Mars has assumed unusual significance and has been a continuing objective for more than 40 years.

The first search for volatile organic compounds (CH_4, C_2H_2, etc.) and other trace species were obtained with the moderate resolution ($\lambda/\Delta\lambda \sim 100$–$1000$) Mariner 9 infrared spectrometer (5–50 μm), obtaining upper-limits for 13 trace species (Maguire, 1977). Accurate and sensitive searches for trace species requires high spectral resolving power ($\lambda/\Delta\lambda > 10{,}000$), but no spectrometer with such resolving power has ever measured the martian atmosphere in the 2–5 μm infrared region (the prime region to search for hydrocarbons and several other species, see Fig. 2) from Mars orbit or from space, heavily restricting access to sensitive measurements of trace molecules (composed of some combination of elements C, H, N, O, P, and S) with possible biological and geochemical origin. By the 1980s, advances in ground-based astronomy permitted sensitive searches for certain sulfur species (e.g., Encrenaz et al., 1991) and other trace gases, including hydrogen peroxide (H_2O_2, Clancy et al., 2004; Encrenaz et al., 2004a, 2012; Hartogh et al., 2010) and methane (e.g., Krasnopolsky et al., 1997). Other advances enabled direct infrared detections of isotopic water (H_2O, HDO; Novak et al., 2002), of ozone (O_3, Espenak et al., 1991) and its proxy ($O_2\,^1\Delta$, Krasnopolsky and Bjoraker, 2000; Novak et al., 2002).

Detection limits improved significantly with the advent of extremely sensitive high-resolution infrared array spectrometers at large ground-based telescopes and advanced data analysis techniques, ultimately permitting the detection of methane (CH_4) in 2003 (Mumma et al., 2009). The recent observations of methane by four groups (Mumma et al., 2009; Formisano et al., 2004; Krasnopolsky et al., 2004; Fonti and Marzo, 2010) indicate regions of localized release, and high temporal variability. The complexity of the observations have prompted questions of the reliability of the detections (Zahnle et al., 2011), but this theoretical work suffers from basic spectroscopic problems (see more details in Section 3.2). The principal plume of the release observed in 2003 contained ~19,000 metric tons of methane, with an estimated source strength ($\geqslant 0.6$ kg s^{-1}, Mumma et al., 2009) comparable to that of the massive hydrocarbon seep at Coal Oil Point (Santa Barbara, CA). By January 2006, the global abundance of methane represented only about 50% of the quantity released in March 2003 (Mumma et al., 2009), suggesting rapid destruction.

The destruction lifetime required to explain the observed decrease in methane abundance (0.5–4 years, Mumma et al., 2009; Lefèvre and Forget, 2009) is much shorter than that predicted by

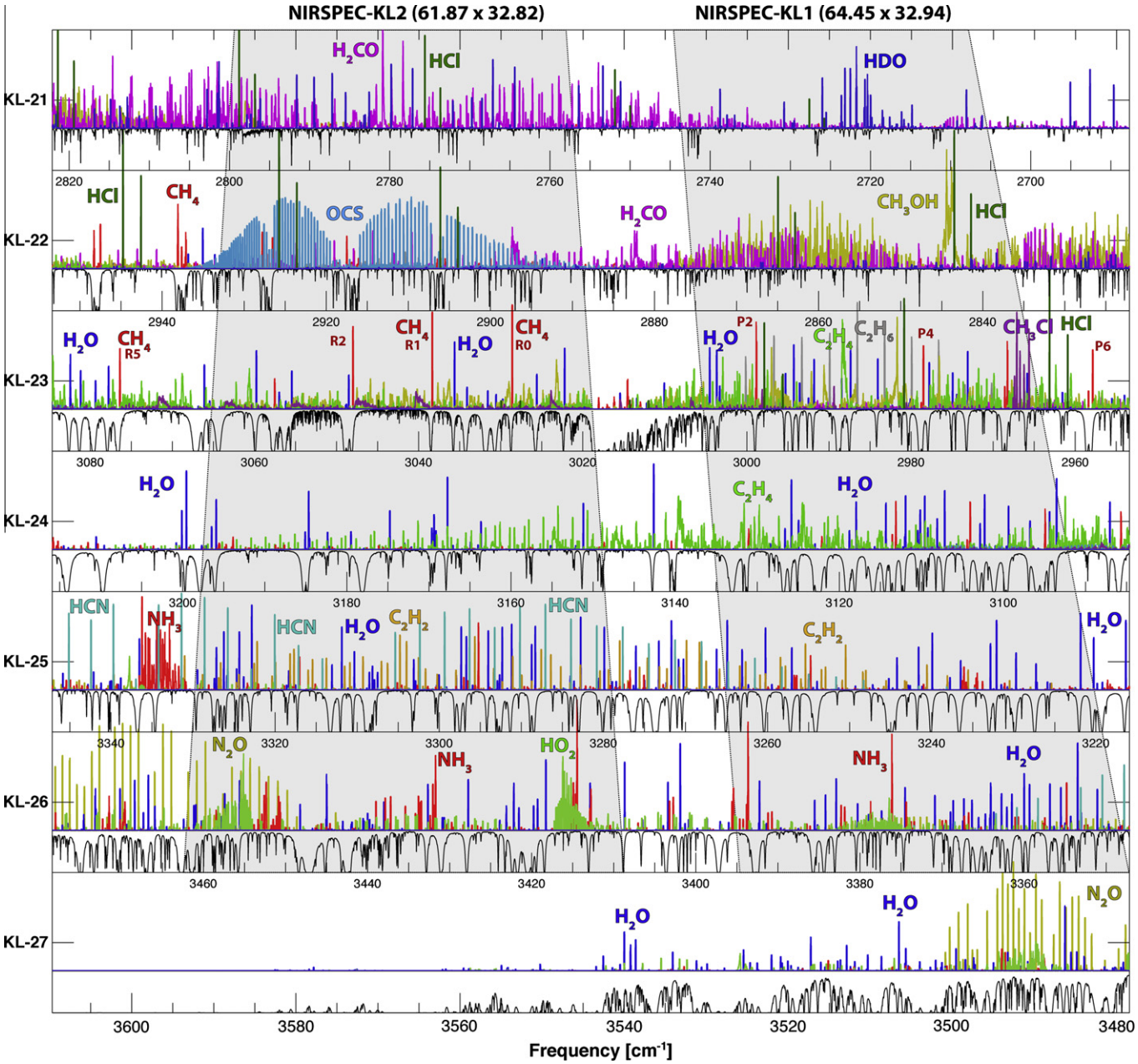

Fig. 2. Spectral simulation of trace species on Mars at infrared wavelengths (K and L bands) accessible using ground-based astronomy and considering a Doppler-shift of +15 km s^{-1}. Atmospheric transmittance from Mauna Kea (4200 m) is shown with a thin black trace. Grayed areas indicate the spectral coverage of the cross-dispersed NIRSPEC/Keck-2 KL1 and KL2 settings.

current photochemical models (centuries, Bertaux et al., 2012; Wong et al., 2004; Krasnopolsky et al., 2004). However, the estimated destruction lifetime is unusually sensitive to the low global abundance measured in 2006, which could be subject to revision. Moreover, little is known about the actual repeatability of the releases, and the release in 2003 could perhaps be consistent with a sporadic event (Mumma et al., 2009; Mischna et al., 2011). A very short destruction lifetime (e.g., 0.5 Earth years) could accommodate annual releases of this size, but a longer lifetime would require fewer or smaller releases each year.

Ultimately, the definitive determination of source regions for the gas requires measurements of its spatial and temporal variations. Isotopic measurements in water co-released with methane will help to constrain the depth of release since the *D*/*H* ratio in permafrost is likely lower considering its preservation over time (Leshin, 2000). Ancient water in Mars meteorites has lower *D*/*H* enrichment than does the current Mars atmosphere (Greenwood et al., 2008; Usui et al., 2012; Villanueva et al., 2012b). Furthermore, a quantitative measure of release rates for methane, and higher hydrocarbons such as C_2H_6, nitrogen and chlorine species, along with sulphuretted species and other gases, would provide a key for assessing biogenic vs. geologic origins (e.g., Allen et al., 2006).

In this paper we present a comprehensive search for trace species on Mars, sampling multiple organic compounds (CH_4, CH_3OH, H_2CO, C_2H_6, C_2H_2, C_2H_4), hydroperoxyl (HO_2), three nitrogen compounds (N_2O, NH_3, HCN) and two chlorine species (HCl, CH_3Cl). Most of these species cannot be detected with current space assets, owing to instrumental limitations (e.g., spectral resolving power). The ~500,000 high-resolution spectra in our ground-based

infrared database sample the molecule-rich infrared spectral region, and present new prospects for detecting many molecules of possible biological and geochemical origin. In particular, the fact that the observations were taken with different instruments and quite different observing conditions allows us to securely identify and isolate sources of systematic error in our measurements. We observed when Mars had both blue and red Doppler shifts, and through terrestrial atmospheric columns (Paranal/Chile, Mauna-Kea/Hawaii) that had very different abundance ratios and temperature/pressure profiles.

In Section 2 we present an overview of our extensive datasets, and details for the datasets included in this paper. The methodology used to analyze the data is presented in Section 3, which includes the realistic modeling of terrestrial atmospheric transmittances, and removal of several instrumental effects, such as scattered light and spectral fringing. Results for all trace species on Mars are presented in Section 4, including a discussion of the methodology we use to derive atmospheric pressures and temperatures. Discussions and conclusions are presented in Sections 5 and 6, respectively.

2. Mars datasets

Searching for gaseous species is most favorable at Near InfraRed (NIR) wavelengths. The 2.8–3.7 μm range encompasses strong fundamental bands for many gases that are accessed with ground-based telescopes (Fig. 2), whose long-slit mapping spectrometers can acquire spectral-spatial maps of multiple gases simultaneously. Above all, several important hydrocarbons – including methane – are symmetric molecules and can only be detected through their ro-vibrational transitions in the NIR since they have no permanent dipole moment and therefore no allowed pure rotational transitions. A Doppler shift is required when searching for species with strong absorptions in our own atmosphere (e.g., H_2O, CH_4, CO), to displace the martian lines from their terrestrial counterparts. The optically thin lines of trace species on Mars are very narrow, and very high spectral resolving power (RP or $\lambda/\delta\lambda \sim 1{,}000{,}000$) is required to measure their intrinsic line shapes. However, lower RP (~30,000) is sufficient to separate the lines of Mars from their terrestrial counterparts at a Doppler shift >12 km/s, and so to measure their equivalent widths. So long as the line shape is not resolved, the measured contrast ratio (line depth relative to continuum intensity) improves with increasing resolving power, leading to improved differentiation among telluric, solar and martian spectral features. We use high-resolution spectrometers (RP > 40,000) at high altitude observatories, to minimize the effects of telluric extinction.

In 2006, we collected 86,000 spectra (68,000 with CSHELL and 18,000 with NIRSPEC) and obtained global coverage. These observations were performed from January 6th to March 3rd (solar longitude L_S = 352–22°), and in this report we present data taken on January 6th 2006 with CSHELL and NIRSPEC (two settings, see Fig. 2) over the same region where Krasnopolsky (2012) recently reported the detection of methane on Mars from observations taken on February 10th 2006. In the 2009–2010 period, we acquired ~400,000 Mars spectra during 27 observing runs (typically three nights per run) using three powerful high-resolution spectrometers (NIRSPEC at Keck II, CRIRES at VLT and CSHELL at NASA-IRTF). From this period, we report results obtained from several representative datasets that span a broad range of seasons, Doppler shifts and spatial coverage (see Table 1), which only represent a fraction of the total search space. The datasets were mainly selected to provide the broadest seasonal coverage possible, but are restricted in their spatial coverage, with a main focus on regions were methane releases have been previously observed. Further results presenting global maps for 2006, 2009 and 2010 will be presented in future publications, now in preparation.

3. Data analysis

The analysis of echelle spectra is relatively complex due to the intrinsic (anamorphic) optical properties of this type of grating instrument, which leads to an irregular mapping of the spatial and spectral dimensions onto the detector array. To process the 2D frames, we developed highly advanced analytical tools that correct for bad-pixels and hits by ionizing radiation, and perform spatial and spectral straightening with milli-pixel precision (Villanueva et al., 2008b). In order to reach maximum sensitivities (photon-noise limited), we also developed new techniques to account for many instrumental effects, such as a thorough characterization of the instrument's response functions, correction for variable resolving power and removal of spectral fringing (using Lomb–Scargle periodogram analysis, Scargle, 1982).

3.1. Removal of telluric features

The terrestrial atmosphere affects the spectra observed at infrared wavelengths in two ways: (1) the raw frames include quantum signatures from Mars and strong terrestrial sky and telescope emissions; at 3.3 μm, the measured martian continuum flux is roughly twice as strong as the telluric background radiance. (2) Radiance from the telescope and the terrestrial atmosphere is removed by nodding the telescope in an A–B–B–A sequence, in which Mars is located at different positions (A, B) along the slit. The A–B frame difference, and the subsequent combination of the A and B martian beams, provides excellent cancellation of sky and telescope emissions. The removal of telluric absorptions is on the other hand extremely complex, and for that purpose we make

Table 1
Observing log and mapping coordinates of the regions sampled on Mars.

Parameter	06 January 2006			19 August 2009	20 November 2009	28 April 2010
Instrument	CSHELL	NIRSPEC KL1	NIRSPEC KL2	CRIRES	CRIRES	NIRSPEC KL2
Time (UT)	05:24	08:39	06:03	10:15	08:26	06:25
	08:16	09:21	06:46	10:30	09:11	08:05
Integration time (mins)	60	24	20	6	40	80
Doppler shift (km s^{-1})	+15.5	+15.5	+15.5	-9.4	-13.8	+15.8
L_S, Mars Year	352°	352°	352°	324°	12°	83°
	MY27	MY27	MY27	MY29	MY30	MY30
Longitude (range)	45W	93W	55W	305W	92W	48W
	85W	100W	66W	315W	99W	67W
Latitude (range)	47N	49N	49N	62N	79N	68N
	78S	80S	80S	63S	45S	30S
Main region	Valles Marineris	East of Tharsis	East of Valles Marineris	Syrtis Major	East of Tharsis	Viking 1 West of Chryse

use of the most advanced radiative transfer models and optimized spectroscopic databases to synthesize a model of the terrestrial absorption. Removal of telluric absorptions derived directly from co-measured spectra of the Moon or nearby stars provides moderate quality residuals, but this method is extremely dependent on atmospheric stability (e.g., water vapor) and observing airmass, ultimately limiting the sensitivity of the measurements. Our approach consists on co-measuring stellar spectra every night, that we use to investigate the instrument's performance during that night and to retrieve the general state of the atmosphere. Martian residuals are derived by removing a synthetic model retrieved for the exact atmospheric conditions at the time of the observations, using as a priori parameters those derived from the stellar spectra (see further details below).

Since 1981, our group has worked with a succession of radiative transfer models for the synthesis of telluric spectra (see discussion in Villanueva et al. (2011)). Initially, we used the Goddard-generated SSP code (Kunde and Maguire, 1974) but transitioned to GENLN2 in 2006 (Edwards, 1992; Villanueva et al., 2006). In 2010, we extensively validated and then integrated the highly robust Line-By-Line Radiative Transfer Model (LBLRTM, Clough et al., 2005) into our data processing methods, and obtained excellent results (e.g., Villanueva et al., 2011, 2012b). LBLRTM is now our preferred model for synthesizing transmittance spectra of Earth and Mars.

Perhaps the biggest challenge of remote sensing of planetary atmospheres is the high degree of incompleteness and frequent inaccuracies contained in current spectral databases. For instance we found that a significant fraction of the C_2H_2, C_2H_6 and NH_3 databases in HITRAN have incorrect frequencies, energies, quantum level assignments, Einstein-A values and statistical weights (e.g., Villanueva et al., 2011; Gordon et al., 2011). These errors occur mainly because empirical databases are a collection of values obtained from diverse investigators, employing different calibration techniques, ultimately giving rise to inconsistencies (see Section 2.1 (H_2O) in Rothman et al. (2009)). Correction and completion of these atlases is particularly complex, and in most cases requires the development of ad hoc quantum mechanical models (as we did for ethane, Villanueva et al., 2011, and methanol, Villanueva et al., 2012a) and the compilation/validation/integration of several spectral databases (as we did for water, Villanueva et al., 2012b). Even though ethane is a trace gas in our atmosphere ($\sim$ 1 ppb abundance), it has a complex spectrum with numerous features overlapping the main spectral region used to search for methane on Mars. Consequently, our new model for ethane enables removal of telluric features in this spectral region with high precision, reaching unprecedented accuracy in the residuals.

3.2. Treatment of telluric isotopologues of methane and water

As we explain in the previous Section 3.1, for the removal of telluric absorption features we synthesize telluric spectra with radiative transfer models and adapt line intensities and spectral parameters from spectroscopic databases. The line intensities for each isotopologue in these databases are scaled from the isotopic ratios used in "standard" laboratory samples. For water the reference is VSMOW (Vienna Standard Mean Ocean Water), while for methane the carbon reference is VPDB (Vienna PeeDee Belemnite). The isotopic composition of the atmosphere on the other hand differs greatly from these standards, and varies along the vertical column. The effect is particularly notable for deuterium depletion (δD) in water, dropping to $-600‰$ at the tropopause owing mainly to preferential condensation of HDO and subsequent rainout (Rayleigh fractionation, cf. Moyer et al., 1996; see Fig. 7 of Villanueva et al. (2012b)). Until recently, no telluric radiative transfer model took this effect into account, and we were first to implement it for water (Villanueva et al., 2012b).

The effect for $\delta^{13}C$ in methane is more subtle. Tropospheric methane is depleted in ^{13}C, with a typical value of $-47‰$ below 20 km owing to its biogenic origin, but its return towards smaller depletion at higher altitudes (Fig. 3B) mainly arises from isotopic discrimination of methane reactions with Cl, OH and O(^{1}D) (Sugawara et al., 1997). The recent claims of Zahnle et al. (2011) when referring to the ground-based searches for methane on Mars by Mumma et al. (2009) are therefore surprising. In particular, they claimed that the ground-based detections of methane may be affected by problems with the treatment of

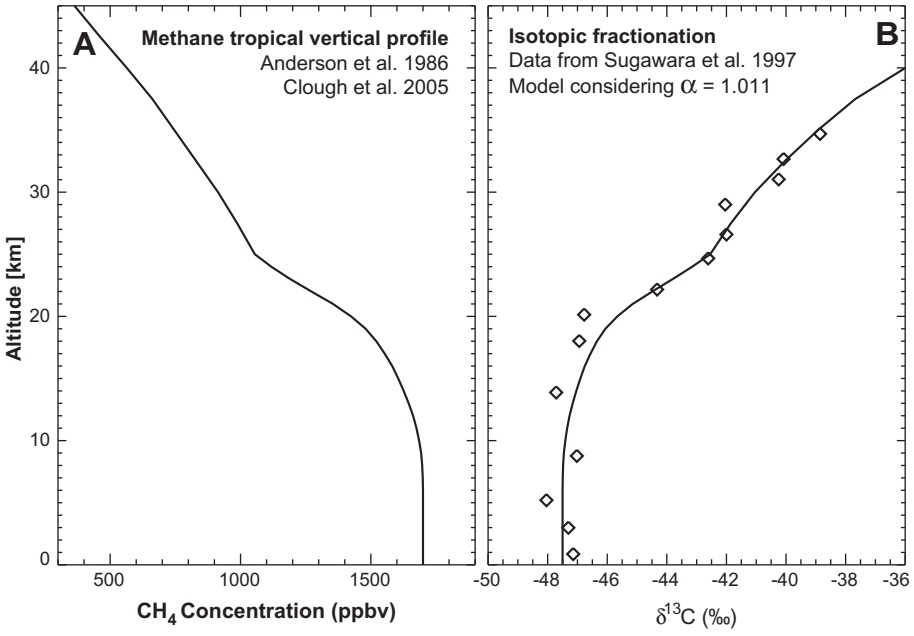

Fig. 3. Methane vertical profile and fractionation curve considered in our terrestrial radiative transfer analysis (see Section 3.2). Diamond symbols in the right-panel present measurements of methane fractionation obtained with a balloon-borne cryogenic sampler (Sugawara et al., 1997). The fractionation model curve was calculated following the Rayleigh distillation equation (e.g., Davidson et al., 1987) with the parameter a set to 1.011.

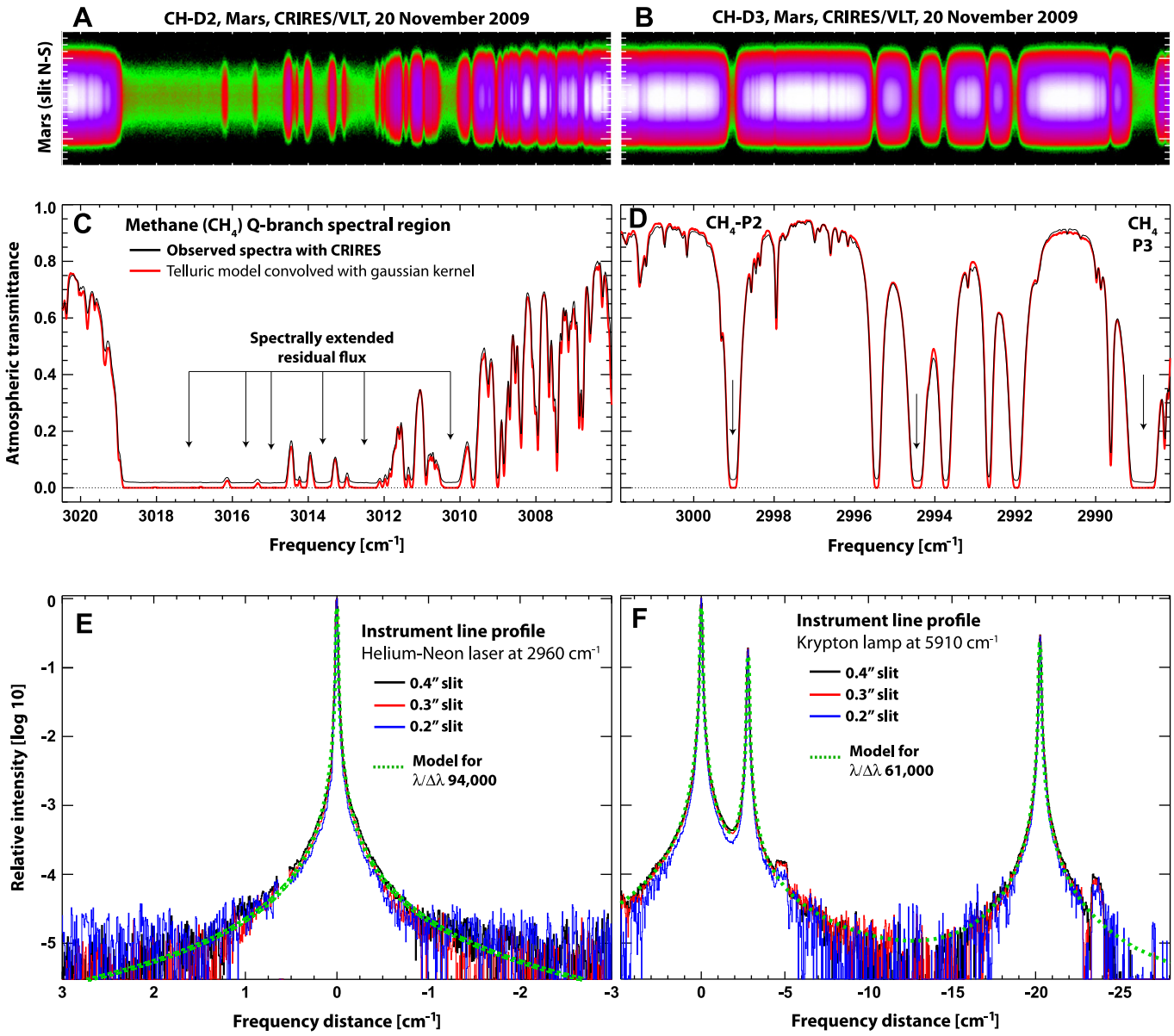

Fig. 4. Instrumental response function of CRIRES/VLT. Panels A–D present infrared echelle measurements of Mars revealing a "residual" light at the core of strong telluric lines, indicate of a grating scattering. Spatial-spectral intensity profiles (A and B) reveal residual intensity in the cores of strong terrestrial lines. Residual flux is indicated by arrows (C and D). Panels E and F show the instrumental response for discrete spectral sources, revealing broad wings, associated with grating scattering. We used these measurements to develop an optical model of the instrument's performance and obtained excellent agreement (dotted lines in panels E and F).

the isotopic lines of methane ($^{13}CH_4$). The issue is that incomplete treatment of the telluric $\delta^{13}CH_4$ in the modeling of telluric spectra would have introduced emissions (not absorptions) in the spectra (Zahnle et al., 2011 agrees), further establishing the Martian detections. If not properly removed, terrestrial $^{13}CH_4$ signatures would appear on the blue wing in our spectra when Mars is red-shifted, but these are not seen (see Fig. S6 of Mumma et al. (2009)).

Moreover, terrestrial effects cannot introduce the gradient in line depths seen along the instrument slit (i.e., increasing with latitude on Mars, from 60°S to 60°N, Mumma et al., 2009). If assigned to a terrestrial signature, the observed increase of the residual line depth along the slit would require the opposite (i.e., positive) signature in $\delta^{13}C$ in telluric methane and an unrealistically large terrestrial isotopic gradient along our slit (Mars was only 7 arcsec on the sky), from +40‰ (60°S on Mars) to +150‰ (60°N on Mars). We remind the reader, that $\delta^{13}C$ in terrestrial methane has been relatively constant (−45‰ to −49‰) over the last 11,000 years in Earth's atmosphere (Sowers, 2010).

Yet, we do believe that a realistic treatment of the distribution of atmospheric methane (and all its isotopologues) is urgently needed, in particular when searching for weak spectral signatures of trace species in planetary atmospheres through ground-based observatories. We have therefore incorporated a realistic vertical profile for both total methane (Fig. 3A) and for $\delta^{13}C$ in methane (Fig. 3B, after Sugawara et al., 1997) into our telluric model, following the methodology initially developed for water in Villanueva et al. (2012b). We note that this minor isotopic effect is diminished owing to two effects: (1) the atmospheric transmittance is small at the (fixed) position of the $^{13}CH_4$ line on the (blue) wing of the $^{12}CH_4$ telluric line, and (2) the isotopic depletion ($\delta^{13}C$) in methane decreases above the tropopause (Fig. 3B).

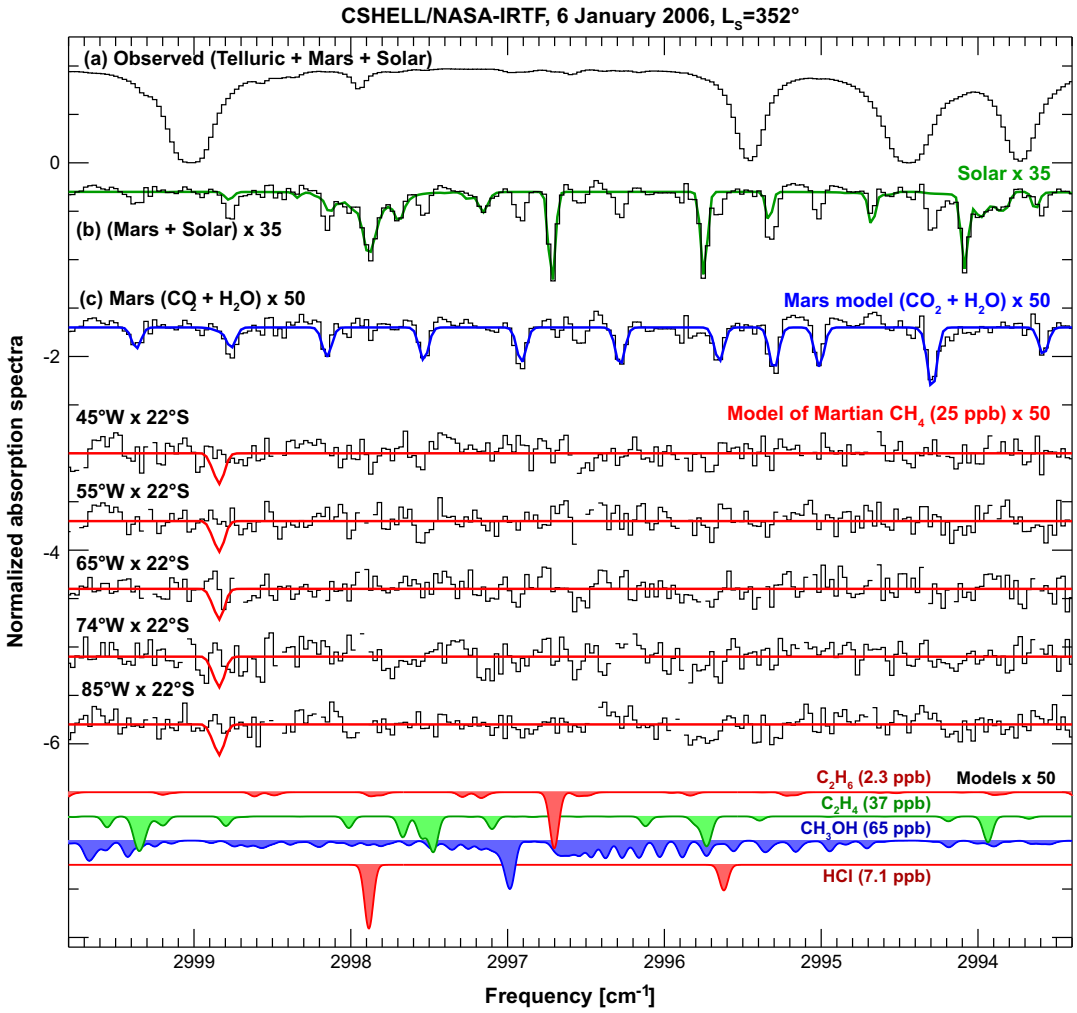

Fig. 5. Sensitive search for methane on Mars over Valles Marineris on January 6th 2006, 1 month prior to the observations by Krasnopolsky (2012) reported up to 25 ppb abundance ratios for methane. Trace 'a' shows the calibrated Mars continuum affected by terrestrial transmittance, and trace 'b' shows the Mars residual spectrum after removing a terrestrial model. Trace 'c' shows the residual spectrum after removing the solar Fraunhofer lines, while the blue trace is a synthetic martian model of CO_2 and H_2O. Our measurements at 22°S latitude in the 45–85°W longitude range reveals no signal of martian methane. Synthetic models for ethane (C_2H_6), ethylene (C_2H_4), methanol (CH_3OH) and hydrogen chloride (HCl) are shown at the 10-sigma detection limit.

3.3. Removal of solar Fraunhofer lines

At near-infrared wavelengths, Mars' spectrum is a combination of reflected sunlight (with Fraunhofer lines) and planetary thermal emission (a featureless continuum; broad spectral features of ices and airborne dust are omitted here). Sparse spectral lines of Mars' atmospheric constituents are superposed on the continua according to the optical path experienced by the two components. Sunlight experiences a double optical path (Sun-to-surface + surface-to-Observer), while the Mars "thermal" continuum traverses only a single path (surface-to-observer). We determine the relative contributions of solar and thermal emission to the measured continuum by comparing the measured area (equivalent width) of Fraunhofer lines with their true value (cf. Novak et al., 2002). This permits identification of the true levels of reflected sunlight and Mars thermal continuum that are needed to correctly determine molecular abundances on Mars. Thus, the accuracy of the solar spectrum has impact not only on the spectral residuals but also on the retrieval process.

To provide an accurate representation of the integrated-disk solar spectrum, we recently combined empirical and theoretical atlases to obtain an improved model for the solar spectrum (see Appendix B of Villanueva et al. (2011)). Our model includes the broadening effects introduced by differential solar rotation and limb darkening, ultimately leading to a highly realistic characterization of the solar features imprinted on the Mars continua (see Figs. 5 and 7–9).

3.4. Instrumental response functions

Convolution of the fully resolved synthetic spectra to match the observed data is a key step to achieve high quality residuals. The response function of grating instruments can be mainly described as a sinc-squared function with very extended wings (see panel E of Fig. 4). The contribution from the wings is normally defined as grating scatter, and has long been recognized to be an important source of systematic error. Cardelli et al. (1990) conducted detailed studies of light scattered from the echelle and cross-disperser gratings in the Goddard High-Resolution Spectrometer developed for HST, and Woods et al. (1994) examined the scattering properties of individual diffraction gratings in detail in preparation for space-borne optics on the Upper Atmosphere Research Satellite and the Total Ozone Measurement Mission. Until recently, the detailed characterization of the instrument response functions of infrared grating spectrometers deployed at ground-based telescopes has been minimal or null, mainly because its measurement

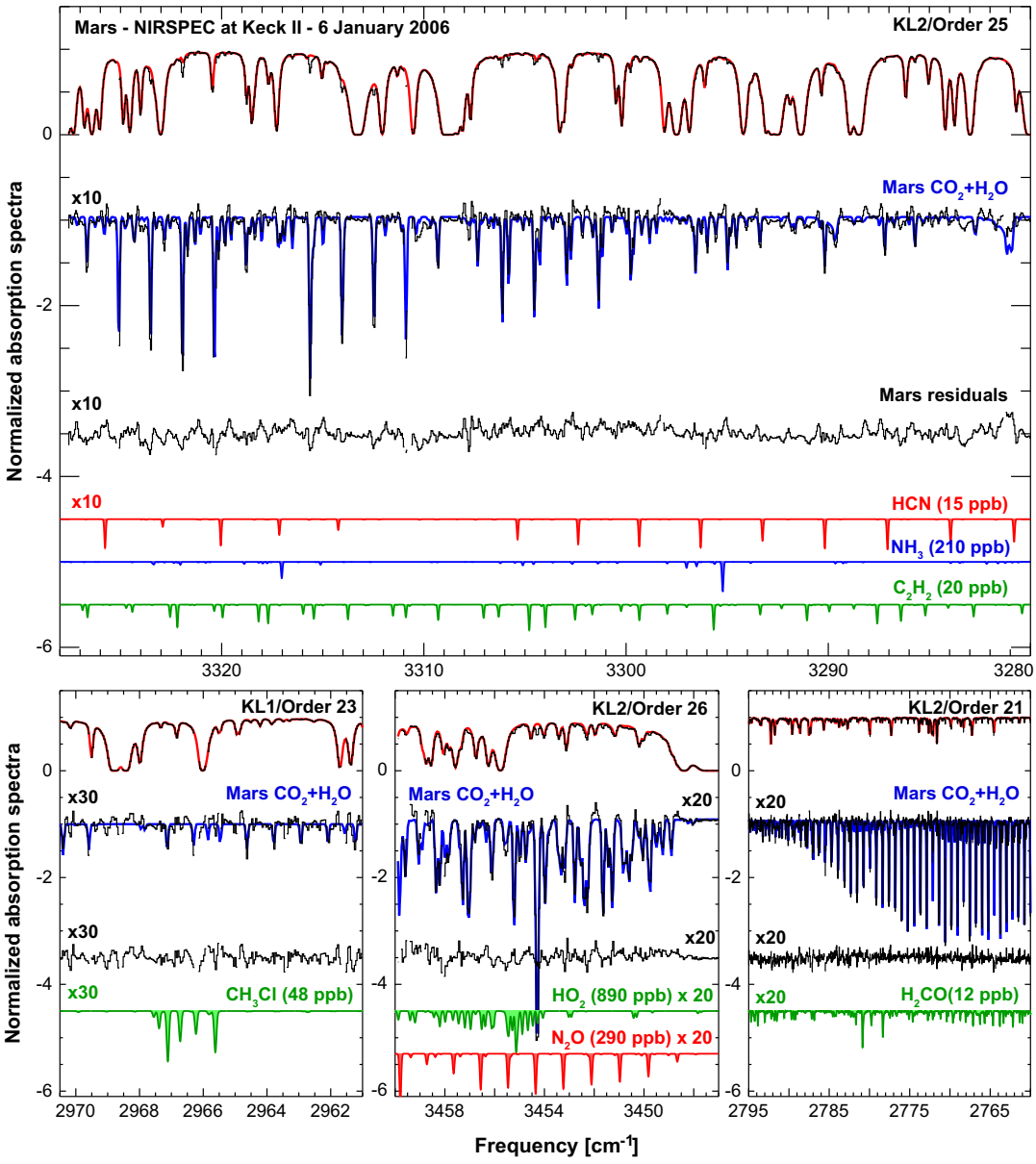

Fig. 6. Search for several traces species with NIRSPEC at Keck on January 6th 2006. Trace descriptions as in Fig. 5.

(and interpretation) requires high signal-to-noise ratio data and high-fidelity processing routines.

We detected residual flux at the core of opaque telluric lines in our CRIRES data (see panels A, B, C and D of Fig. 4) by performing a careful study of the instrument's response to the Mars signal using our advanced analytical routines (see Fig. 4). In order to properly characterize this effect, we fed CRIRES with two discrete spectral sources (Helium–Neon laser and Krypton lamp), and investigated the instrument's response function in the 1–4 μm region. The collected spectra feature extremely high signal-to-noise ratio, and allowed us to detect the broad wings of the response function that are five orders of magnitude weaker than the peak signal. These measurements are particularly applicable to observations of extended objects (e.g., Mars) since the spectral lamps fill the slit, and therefore comparisons to Mars data are more immune to the possible inclination between straylight and dispersion directions (see spectral library by Lebzelter et al. (2012)).

By measuring the response function at different slit-widths, we determined that the morphology of the wings did not change substantially, while the core resolving power did. Using the 0.2 arcsec slit, we measured a resolving power of 94,000 at 3.3 μm, while the 0.3 arcsec delivered a resolving power of 60,000 (similar to the findings of Siebenmorgen (2007) at 2.2 μm). On the other hand, the morphology of the wings did not change substantially (see Fig. 4E and F) for the three slits. By creating a "straw-man" model of the optical systems of CRIRES, we managed to reproduce the morphology of the instrumental response function (see dotted lines in panels E and F of Fig. 4).

Most importantly, we determined that the shape of the wings to be mainly defined by the quality and precision of the echelle grating. The effect of the "wings" on the observed spectra is to introduce a spectrally extended residual flux, particularly evident at the core of optically thick terrestrial lines. If omitted from our analysis methods by simply convolving with a Gaussian kernel, this effect would restrict the maximum achievable signal-to-noise ratio to ~150 for absolute retrievals in the 3.3 μm spectral region. Using the response functions presented in Fig. 4, we created a set of instrumental response functions that replicate the observed

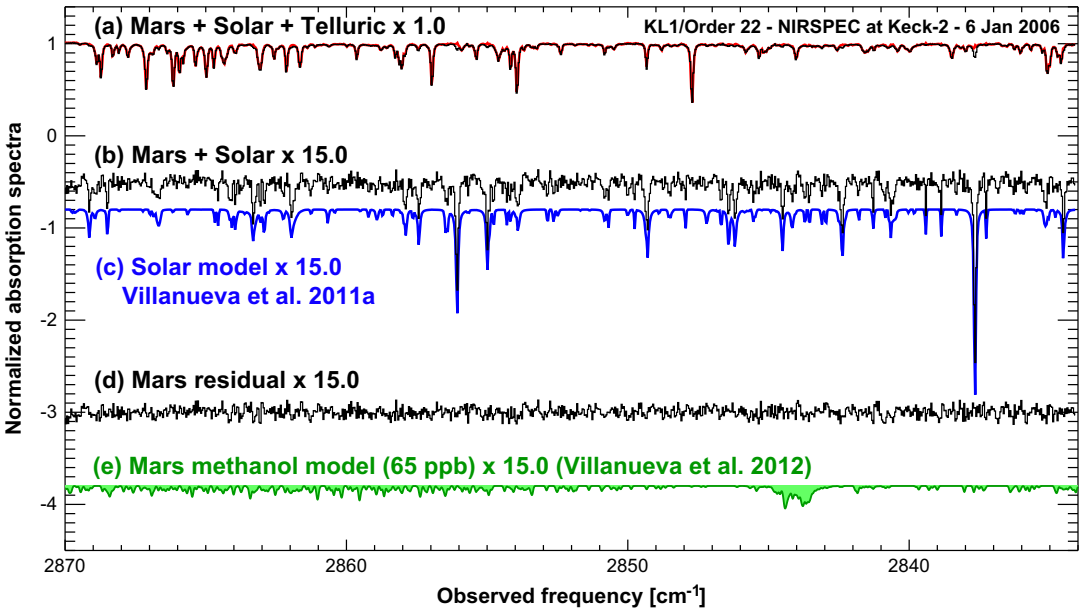

Fig. 7. Mars infrared spectrum taken on January 6th 2006 with NIRSPEC at Keck-II. Trace 'a' shows the calibrated Mars continuum affected by terrestrial transmittance, and trace 'b' shows the Mars residual spectrum after removing a terrestrial model. Trace 'c' shows the solar spectrum synthesized using our newly developed methodology (Villanueva et al., 2011), while trace 'd' shows the residual spectrum after removing this solar model. We derived a sensitive upper limit for CH_3OH on Mars by integrating over the Q-branch of trace 'd' at 2844 cm^{-1}.

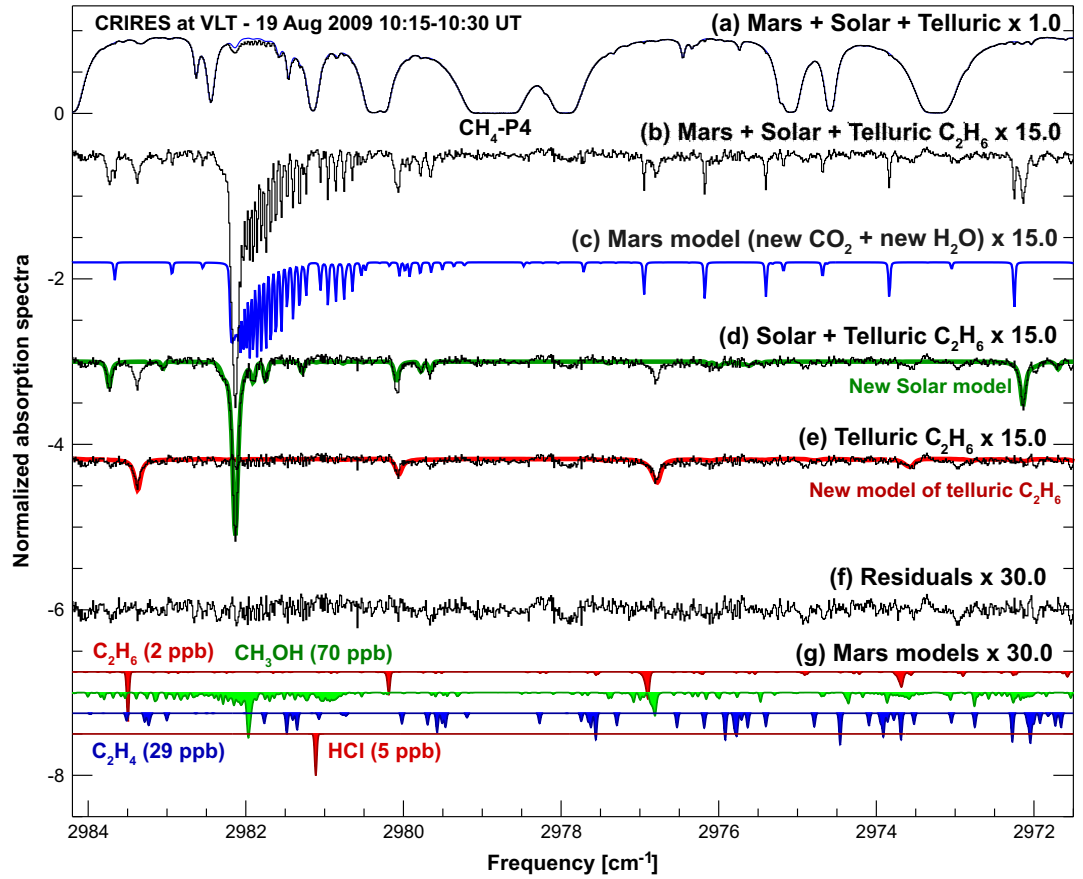

Fig. 8. Retrieval of sensitive upper limits for ethane (C_2H_6), methanol (CH_3OH) and ethylene (C_2H_4) on August 19th 2009 using CRIRES at VLT. Trace 'a' shows the calibrated Mars continuum affected by terrestrial transmittance, and trace 'b' shows the Mars residual spectrum after removing a terrestrial model (without telluric ethane). Trace 'd' shows the residual spectrum after removing a Mars model of CO_2 and H_2O (trace 'c'). Solar lines are observed in the solar residual (trace 'd'), while the detection of telluric ethane lines is shown in trace 'e'. After removing solar lines and telluric ethane lines using our new models (Villanueva et al., 2011), we derive the final residual spectrum, presented as trace 'f' (now multiplied by 30). From this residual spectrum, we derived sensitive upper limits for C_2H_6, CH_3OH, C_2H_4 and HCl.

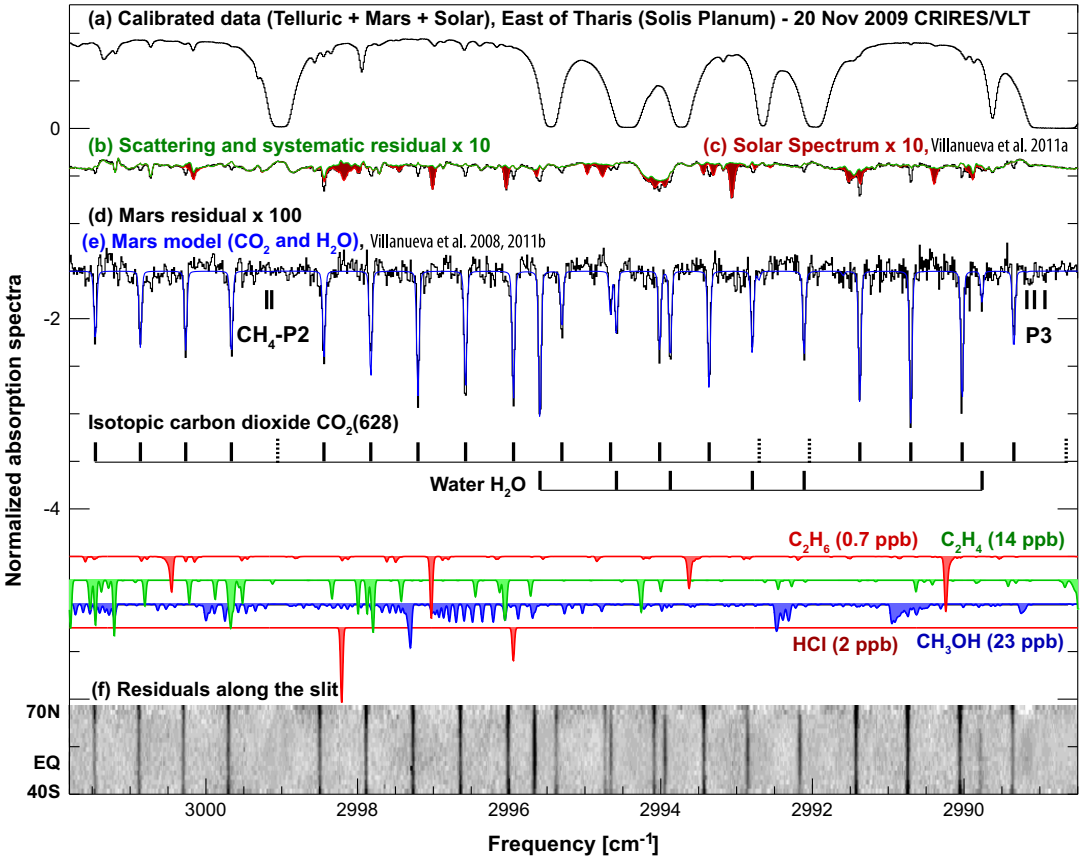

Fig. 9. Detection of water (H_2O) and isotopic carbon dioxide CO_2 (628) on Mars on November 20th 2009 using CRIRES at VLT. Trace 'a' shows the calibrated Mars continuum affected by terrestrial transmittance, and trace 'b' shows the Mars residual spectrum after removing a terrestrial model. The green trace shows the scattering and systematic residual obtained by computing a synthetic residual with the kernels in Fig. 4 and by comparing to co-measured stellar spectra (see Section 3.4). Trace 'd' shows the residual spectrum after removing the solar Fraunhofer lines (trace 'c'), while trace 'e' is a synthetic martian model of CO_2 and H_2O. Residual spectra from 70°N to 40°S are presented in panel F (grey scale format). The R24 line of CO_2 628 is extinguished by terrestrial methane P2 (compare spectra in A, E, F near 2999 owing to the lower RP cm^{-1}). In panel F, note the low abundance of H_2O above 30°N at this season (very early spring, Northern hemisphere), e.g. lines near 2993.95, 2989.8 cm^{-1}. (For interpretation of the references to color in this figure legend, the reader is referred to the web version of this article.)

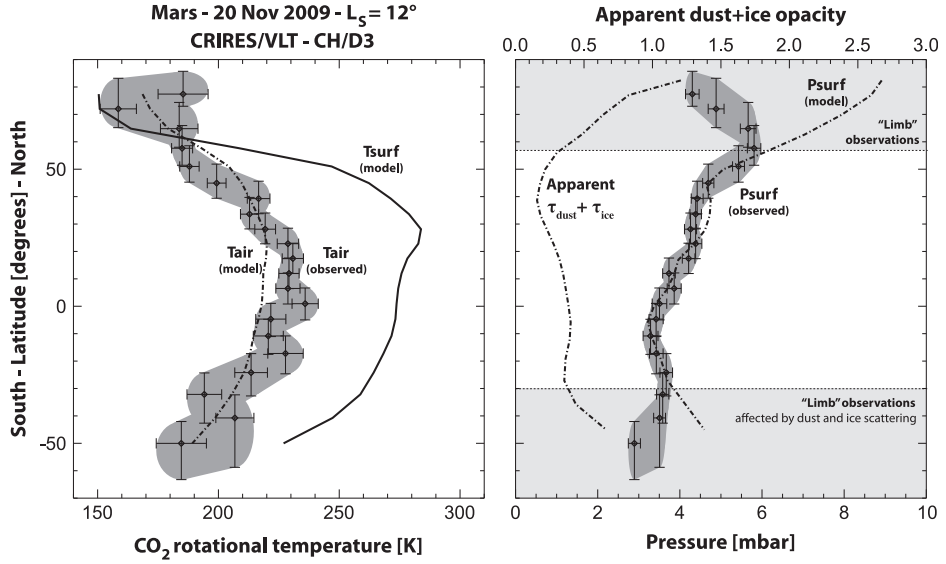

Fig. 10. Retrieval of rotational temperature and surface pressure from the spectral extracts presented in Fig. 9. The effects of dust and ice scattering are particularly significant at high observing angles ("limb" observations).

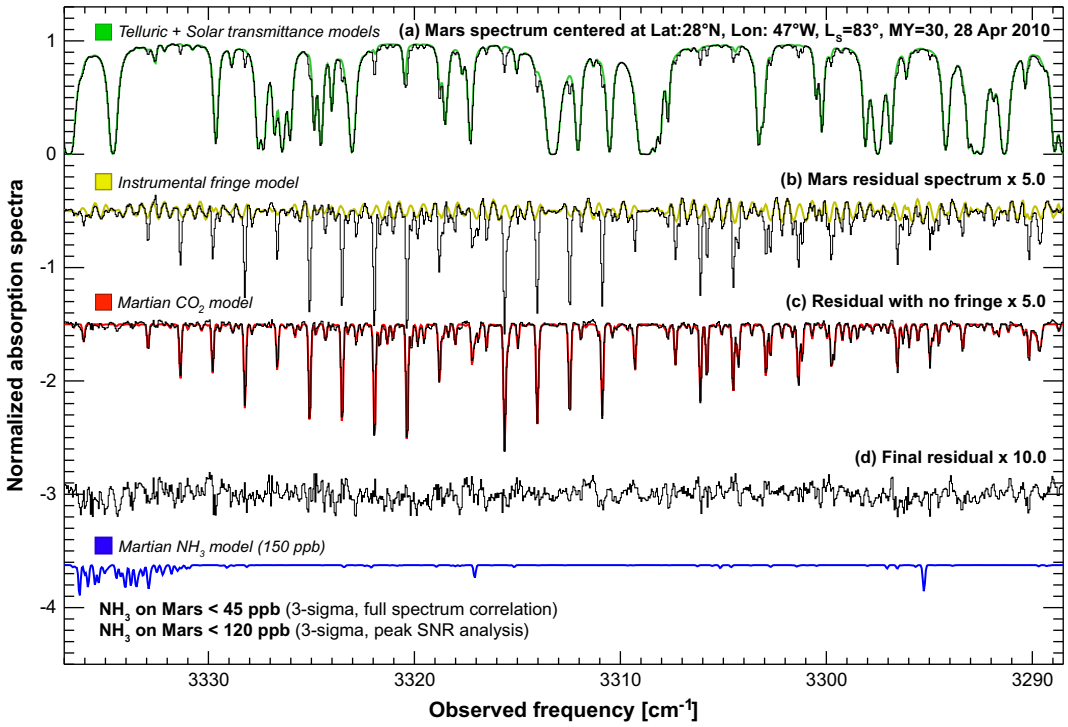

Fig. 11. Sensitive search for ammonia (NH_3) on Mars on April 28th 2010 using NIRSPEC at Keck-2. Trace 'a' shows the calibrated Mars continuum affected by terrestrial transmittance, and trace 'b' shows (multiplied by 5) the Mars residual spectrum after removing a terrestrial model. Trace 'c' shows (multiplied by 5) the residual spectrum after removing a model of spectral fringing, showing strong martian CO_2 absorptions. Trace 'd' shows the final residual (multiplied by 10) after removing a model martian CO_2. From this residual spectrum, we derived a sensitive upper limit for NH_3.

Table 2
Abundance limits (3-σ) of trace species on Mars in parts-per-billion (ppb, 10^{-9}).

Molecule	Previous (3-σ, ppb)	06 January 2006 L_S 352° MY27	19 August 2009 L_S 324° MY29	20 November 2009 L_S 12° MY30	28 April 2010 L_S 83° MY30
Methane (CH_4)	3–50[a]	<7.8	–	<6.6	<7.2
Ethane (C_2H_6)	<0.2–0.6[b]	<0.7	<0.6	<0.2	–
Methanol (CH_3OH)	–	<19	<21	<6.9	–
Formaldehyde (H_2CO)	<4.5[c]	<3.9	–	–	<3.9
Acetylene (C_2H_2)	<3[d]	<6	–	–	<4.2
Ethylene (C_2H_4)	<750[d]	<11.2	<9	<4.1	–
Nitrous oxide (N_2O)	100[d]	<87			<65
Ammonia (NH_3)	<8[d]	<57	–	–	<45
Hydrogen cyanide (HCN)	–	<4.5	–	–	<2.1
Methyl chloride (CH_3Cl)	–	<14.3	–	–	–
Hydrogen chloride (HCl)	<0.3[e]	<2.1	<1.5	<0.6	–
Hydroperoxy radical (HO_2)	–	<198	–	–	<255

[a] Mumma et al. (2009), Krasnopolsky et al. (2004), and Formisano et al. (2005).
[b] Villanueva et al. (2011) and Krasnopolsky (2012).
[c] Krasnopolsky et al. (1997).
[d] Maguire (1977).
[e] Hartogh et al. (2010).

spectra. This technique combined with co-measurements of stellar spectra allowed us to achieve extremely high signal-to-noise ratio in the reduced residual spectra for Mars (e.g., Figs. 8 and 9).

3.5. Removal of instrumental spectral fringing

Spectral fringes arise from multiple reflections between two optical surfaces, and interference of the resulting wave fronts. The fringe spacing is 1/nL, ('n' is the index of refraction in the medium, and L is the separation of the two surfaces). For NIRSPEC, the main measured fringe spacing is 0.57 cm^{-1} (Fig. 11), while the infrared detector has '*n*' of ~4, which would correspond to a spacing of 4.4 mm between the optical surfaces. The combination identifies the detector itself as the fringe-forming medium. CRIRES does not show notable fringing, while CSHELL has a main fringe with a spacing of 1.2 cm^{-1}, corresponding to an optical spacing of 2.1 mm. Minor echelle movements, thermal flexing, mechanical stress, etc. introduce small shifts in the wavelength mapping onto the detector and displace slightly the fringe pattern of the data and calibration exposures. The process of flat fielding, a non-linear

multiplicative operation, would produce a whole new set of harmonics, all related to the intrinsic optical spacing.

We correct for spectral fringing as follows. We first perform a Lomb–Scargle periodogram analysis on the residual spectra (e.g., trace b, Fig. 11), from which we obtain the parameters (period, amplitude and phase) of the three strongest periodic features. Next, we multiply each synthetic periodic signal by the atmospheric transmittance and subtract the product function from the residual spectra pixel-by-pixel. The results of this procedure provide excellent removal of fringe signatures, creating a corrected residual spectrum dominated by true signatures of trace gases on Mars (e.g., trace c, Fig. 11).

4. Characterization of the martian atmosphere

4.1. Volatile organic compounds (VOCs) on Mars

On Earth, atmospheric volatile organic compounds (VOCs: CH_4, C_2H_6, CH_3OH, H_2CO, etc.) arise mainly from biogenic and anthropogenic emissions, and therefore these species are normally considered indicators of life (making them so-called "biomarkers"). Many of these species are short-lived in the martian atmosphere, and thus they disappear shortly after their release—within hours for H_2CO, and days for C_2H_6 and CH_3OH (Wong et al., 2004). These short-lived species therefore track current activity. On the other hand, methane (CH_4) has a relatively long column lifetime on Mars (the 3D model of Lefèvre and Forget (2009) predicts $\tau \sim 300$ Earth-years), and any seasonal or periodic releases of methane will lead to its accumulation over time, increasing the chances for its detection. If detected, the abundance ratios of short-lived species can assist in testing the manner of their release, and their predicted persistence lifetimes. Upper limits can also provide useful constraints on these parameters, if sufficiently sensitive.

The column lifetime of methane is so long because oxidation by OH and $O(^1D)$ is relatively slow ($\tau > 600$ years, Nair et al., 2005), and UV photolysis of methane is shielded by CO_2 below ~70 km (Wong et al., 2004; Bertaux et al., 2012). [At 70 km, the methane photolytic lifetime is only ~7 Earth-days (Bertaux et al., 2012).] Vertical mixing thus controls the rate of destruction for column methane. The methane column lifetime could be reduced to only 44 years if the strong vertical transport inferred at polar latitudes occurred everywhere on the planet, and at all seasons (Bertaux et al., 2012). However, Bertaux et al. noted that recycling of the atmosphere at high altitude seems far too slow to significantly reduce the nominal column lifetime (~300 years) of CH_4. Once methane is destroyed via photolysis (yielding CH, CH_2 and CH_3) or via oxidation (producing CH_3), subsequent chemical reactions produce many additional infrared-active trace gases (Fig. 1), including CH_3OH, H_2CO, and C_2H_6 (the latter via CH_3–CH_3 recombination, Wong et al., 2004).

Aside from photochemistry, terrestrial ethane and higher alkanes are produced efficiently by thermogenesis in subterranean traps. Microbial studies demonstrate that C2 and higher alkanes are not produced efficiently by bioprocesses. By analogy, the CH_4/C_2H_6 abundance ratio on Mars can test photochemistry, but can also constrain microbial vs. thermogenic origins (Horita and Berndt, 1999; Allen et al., 2006). Consequently, measurements of the abundance ratios of VOC species (along with their temporal and spatial distributions) are critically needed to fully characterize their sources and sinks on Mars, and to further test the chemical pathways of these species in the martian atmosphere.

4.2. Methane (CH_4)

Four groups report detections of methane on Mars (see Section 1), with mixing ratios in the 3–70 ppb range. Recently, Krasnopolsky (2012) claimed a detection (8-σ) of the CH_4 R0 (ν_3) line on 2 February 2006, implying a peak abundance of 25 ppb at 20°S and 70°W (near Coprates Chasma, Valles Marineris). The season was vernal equinox ($L_S = 5.6°$). The observed plume had a FWHM of ~40° equivalent to an area of $\sim 4.5 \times 10^6$ km^2 and sampled 9.9×10^{39} molecules, when considering the mean martian column density of 2.2×10^{33} molecules km^{-2} (see SOM-4 of Mumma et al. (2009)). A plume of 25 ppb would then correspond to 2.5×10^{32} molecules (6600 metric tons) of methane.

In the same season (January and February 2006), we conducted extensive searches for CH_4 and other trace species on Mars with CSHELL at IRTF and NIRSPEC at Keck II. Results for the Eastern hemisphere were presented in Mumma et al. (2009). Here, we present results obtained on 6 January 2006 from high-quality data over the same region sampled 4 weeks later by Krasnopolsky (2012). We searched the CH_4 P2 (ν_3) line at 2999 cm^{-1} (see Fig. 5), but did not detect any sign of Mars methane in our spectra (our upper limit is <7.8 ppb (3-σ), or <2100 metric tons). If Krasnopolsky's claimed detection is correct, at least 4500 metric tons were released in a span of 27 days or less, with a mean outgassing rate of at least 2 kg s^{-1}. When including atmospheric transport in this estimation (e.g., Lefèvre and Forget, 2009; Chizek et al., 2010), the combined source strength required for the detections by Krasnopolsky (2012) would be at least an order of magnitude stronger, which is quite extraordinary.

In orbit, methane abundances with MEX/PFS from January/2004 ($L_S = 330°$, MY26) to March/2010 ($L_S = 60°$, MY30) indicate extremely high spatial and seasonal variability with peak abundances near 60 ppb (Geminale et al., 2011). These measurements sample the ν_3 Q-branch at 3018 cm^{-1} (3.3 μm). Methane maps obtained by sampling the ν_4 Q-branch at 1305 cm^{-1} (7.7 μm) with MGS/TES from March/1999 ($L_S = 103°$, MY24) to August/2004 ($L_S = 103°$, MY24) show substantially different spatial and seasonal variability with peak abundances near 70 ppb (Fonti and Marzo, 2010). Our individual methane upper-limits (<7 ppb, see Tables 1 and 2) obtained from January/2006 ($L_S = 352$, MY27) to April/2010 ($L_S = 83$, MY30) are generally smaller than the seasonal values reported by these works. Considering the complexities associated with measuring methane at the low spectral resolutions featured by MGS/TES and PFS/MEX, those measurements may be affected by instrumental effects (e.g., micro-vibrations) and unrecognized solar/water signatures, that dominate the spectral regions used by these teams to search for methane.

By contrast, the fact that we observe a featureless residual spectrum (after removing all known telluric, solar and martian lines) over a large number of pixels (Fig. 5) further validates the analytical methods used to derive our upper limits (non-detection) from high-resolution spectra. In summary, our non-detections at vernal equinox (February 2006, Mumma et al., 2009; and November 2009, this work) and late Northern spring (April 2010, this work) further strengthen the possibility of non-seasonal release of methane (see Table 1). If methane is being released into the atmosphere, this process is probably sporadic and not continuous.

4.3. Methanol (CH_3OH) and formaldehyde (H_2CO)

The detection of CH_3OH and H_2CO on Mars would conclusively establish the existence of a VOC chemical network on Mars, and most importantly would point to regions of active release on the planet. On Earth, biogenic sources produce huge quantities of methanol ($\sim 2.70 \times 10^{14}$ g/year) – about 1/3 the mean value of methane production – and thus these two gases represent (respectively) 6% and 23% of biogenic VOC emissions (Fall, 1999; Heikes et al., 2002). The mean free tropospheric abundances for these two species on Earth are, on the contrary, extremely different (0.6 ppbv for CH_3OH and 1800 ppbv for CH_4), reflecting the much

shorter column lifetime of methanol (9 days) with respect to that of methane (8 years). Nevertheless, methanol is one of the most abundant volatile organic compounds (VOCs), and it provides a significant source of tropospheric carbon monoxide (CO) and formaldehyde (H_2CO) (Xiao et al., 2012, and refs. therein). Formaldehyde is mainly produced by photochemistry in our atmosphere, and has peak abundances lower than 10 ppb (Luecken et al., 2012). On Mars, the photochemical lifetimes of H_2CO and CH_3OH are extremely short (7.5 h and 74 days, respectively), leading to extremely low predicted abundances ($\sim 10^{-6}$ ppb for both) if CH_3OH and H_2CO are produced solely from CH_4 oxidation (Wong et al., 2004). On the other hand, regions of active biogenic release on Mars could show abundances comparable to that of methane, by analogy with terrestrial systems (Fall, 1999; Heikes et al., 2002).

The search for formaldehyde on Mars has a checkered history. At equatorial latitudes in Mars' early spring (February–March 1989; L_S range 1.6–18.5°), Korablev et al. (1993) acquired infrared spectra in solar occultation from the Mars-orbiting Phobos spacecraft. They detected two new absorption features (at 2710 and 2730 cm^{-1}), attributed them to H_2CO, and retrieved an abundance ratio of 0.5 ppm (+0.8/−0.3). Re-analysis of the data (Korablev, 2002) led to improved martian residuals after correcting for non-linearity problems and periodic deformations, confirming the reality of these two features (2710, 2730 cm^{-1}) which remained in the re-analyzed spectra. The authors were puzzled by these extremely high H_2CO abundances, and ultimately concluded that these features probably originated from some unknown instrumental problem. Interestingly, in 2008 we discovered a new band of (doubly-substituted) isotopic carbon dioxide (638) centered at 2702 cm^{-1} (Villanueva et al., 2008a, see revised molecular constants in Table A1 of Villanueva et al. (2011)). Their 2710 cm^{-1} "feature" could then correspond to the R-branch of this band system. Considering that the martian atmosphere is composed mainly of CO_2 (95%), we can disregard the previous attribution of the features observed by Phobos, and securely conclude that formaldehyde was not present in 1989 (Korablev et al., 1993). Investigations based on high-resolution ground-based spectra in this same spectral region returned much smaller upper limits for H_2CO. Using spectra acquired on 28–30 June 1988 (L_S = 222–223°; mid-spring in Mars' Southern hemisphere), Krasnopolsky et al. (1997) reported an upper limit (<4.5 ppb, 3-σ). Our searches for H_2CO in 2006 and 2010 returned upper limits <3.9 ppb (see Table 1 for dates and seasons).

Measurements of methanol (CH_3OH) on Mars have been more elusive, probably because of the lack of spectroscopic databases for this complex molecule – methanol has a hindered internal rotation and asymmetric structure. We recently constructed a line-by-line model for the ν_3 band of methanol at 2844 cm^{-1} (3.52 μm, Fig. 7) by characterizing each torsional K-ladder with a set of unique rotational constants including a practical approximation of the three torsional modes of the vibrational levels (Villanueva et al., 2012a). Using the same technique and considering the line assignments reported by Xu et al. (1997), we also created a quantum band model for the ν_2 band of methanol at 2999 cm^{-1} (3.33 μm) and applied it to our Mars data (Figs. 5, 8 and 9). Using these newly developed spectroscopic databases, we report the first upper limit for this trace gas on Mars, with an abundance ratio <7 ppb (3-σ, Table 2).

If we adopt the terrestrial biogenic production ratio ($CH_4/CH_3OH \sim 3$) for Mars, our sensitive upper-limits for these two species (ppb-levels, see Table 2) demonstrate that there was no concurrent active release from biogenic sources at the regions sampled in 2006, 2009 and 2010 (see Table 1). The mixing ratios for methanol and formaldehyde would be $<10^{-6}$ ppb if produced solely by photochemistry of quiescent atmospheric methane, and thus our upper limits for CH_3OH (<7 ppb) and H_2CO (<4 ppb) do not provide critical tests of photochemical production, considering the <7 ppb limit derived by us for CH_4 (Table 2).

4.4. Alkanes (ethane, C_2H_6), alkenes (ethylene, C_2H_4) and alkynes (acetylene, C_2H_2)

Measurements of ethane and any other high n-alkane hydrocarbon gases can be used to distinguish between different types of active regions (e.g., biology vs. geology). On Earth, thermogenic sources typically contain comparable amounts of ethane and methane ($CH_4/C_2H_6 < 50$), while microbial degradation typically produces only methane ($CH_4/C_2H_6 > 1000$, Bernard et al. (1976) and refs. therein). Furthermore, alkanes, alkenes and alkynes are normally very short-lived (e.g., the column lifetime for C_2H_6 is only 25 days on Mars, Wong et al., 2004), so these would point directly to regions of active release. None of these species has been detected previously, and the predicted ambient abundances for these species are extremely low if they are solely produced photochemically from methane (Wong et al., 2004).

The first search for ethane was performed by Maguire (1977), who derived an upper limit of 400 ppb from globally averaged spectra obtained by low resolution infrared spectra acquired by the IRIS spectrometer on the Mariner 9 spacecraft. Instrumental sensitivities have improved greatly in recent years, with Villanueva et al. (2011) reporting an abundance ratio <0.6 ppb (3-σ), and Krasnopolsky (2012) reporting a limit of 0.2 ppb. Our upper limit presented in 2011 and those presented in Table 2 (<0.2 ppb) make use of our new quantum mechanical model for the ν_7 band of ethane centered at 2985 cm^{-1} (3.3 μm), that contains 8680 spectral lines and a novel description of the torsional hot-band component ($\nu_7 + \nu_4 - \nu_4$). We also searched for the simplest alkene (C_2H_4) and alkyne (C_2H_2), at 3.3 μm and 3.0 μm respectively, obtaining very sensitive upper limits (<6 ppb, see Table 2).

4.5. Odd-hydrogen species: Hydroperoxyl (HO_2)

Since CO_2 photolysis ($CO_2 + h\nu \rightarrow CO + O$) is much faster than the 3-body formation reaction ($CO + O + M \rightarrow CO_2 + M$), one would expect the atmospheres of Mars and Venus to be dominated by CO and O_2, if no other mechanisms were in play (Stock et al., 2012a,b). In the early 1970s, it was quickly realized that reactions catalyzed by odd-oxygen (O_x: O and O_3) and odd-hydrogen (HO_x: H, OH and HO_2) molecules permitted the existence of a stable CO_2 atmospheres on Mars and Venus (e.g., McElroy and Donahue, 1972). Radical species, such as HO_2, are expected to have low abundances, but since HO_2 takes part in the chemical pathways of the main atmospheric constituent (CO_2), its abundance is still among the top 20 species on Mars. There are no direct measurements of odd hydrogen (OH, HO_2) on Mars, so even upper limits can be of key importance for testing this hypothetical pathway for stabilizing the martian atmosphere (Fig. 1).

The predicted spectrum of HO_2 is extremely complex (Figs. 2 and 6), and the absorption intensity is spread over a broad range of frequencies (or wavelengths), making its detection particularly challenging. Our 3-sigma upper limits indicate abundances lower than 200 ppb (Table 2), which are consistent with the 0.1–6 ppb range predicted by current 3D chemical models (e.g., Lefèvre et al., 2004) but do not meaningfully test the models. Future detections of this short-lived trace gas will require measurements using other techniques (e.g., Herschel/HIFI, solar occultation measurements from Mars orbit) or via ad hoc enrichment chambers (e.g., as for CH_4 onboard the Mars-Science-Laboratory).

4.6. Nitrogen compounds (N_2O, NH_3, HCN)

Molecular nitrogen (N_2) is the second most abundant gas in the martian atmosphere with a mean abundance of 2.7%, but the sources and sinks of nitrogen are poorly known. N_2 is the expected main reservoir of N-atoms in the atmosphere, with any NH_3 and

N_2O being quickly photolyzed. A large amount of primordial nitrogen was lost via non-thermal escape to space as evidenced by the enriched $^{15}N/^{14}N$ ratio measured by Viking (McElroy et al., 1976; McKay and Stoker, 1989).

Mancinelli and Banin, 2003 predicted that nitrogen stored as salts in the regolith could exceed the present atmospheric content by a factor of 1000. Any abiotic or biological process in contact with these nitrate salts could lead to the production and release of N_2O, and therefore its presence is a direct indicator of recent release from a sub-surface source. If ammonia (NH_3) is present in the sub-surface, it could permit water to be in the liquid form at moderate depths. Any evidence of HCN would indicate that the release is related to primordial material, since HCN is not expected to be produced in a CO_2 atmosphere (Mancinelli and Banin, 2003). Here, we derive the most sensitive upper limits achieved to date for N_2O (<90 ppb) and HCN (<5 ppb), and sensitive values for ammonia (NH_3) of <60 ppb. Our upper limits are consistent with current predictions of photochemical models for Mars (Krasnopolsky, 1993) that assume simple recycling of N_2 molecules (see Fig. 1) and no active release of nitrogenated gases.

4.7. Chlorine species (HCl, CH_3Cl)

Chlorine chemistry can play a significant role in terrestrial atmospheres. On Venus, the stability of its dense CO_2 atmosphere is controlled by chlorine atoms (Cl) derived from the photolysis of HCl (Yung and Demore, 1982). On Mars, this important catalytic role is played primarily by odd-hydrogen species, such as OH and HO_2 (Section 4.5). If chlorine chemistry is active at any level in the martian atmosphere, the principal gaseous forms should include HCl (the principal reservoir species), ClO, ClO_2, HOCl, ClCO, $ClCO_2$, and even CH_3Cl (if organics are present, see below). For these chemicals to be active on Mars today, some injection of chlorine from the surface is required. Their detection could identify and constrain a cycle of chlorine exchange between the surface and atmosphere. Two chlorinated species have strong vibrational bands in the spectral region sampled by us, HCl and CH_3Cl.

On Mars, the first measurements of elemental chlorine (Cl) in the soil revealed relatively high concentrations (~0.7 wt%) at the Viking 1 landing site (Chryse Planitia, Clark et al., 1976). Similar concentrations were found in other regions on Mars by the Pathfinder, Spirit and Opportunity rovers, with a typical Cl abundance of ~0.6 wt% (Rieder et al., 1997; Gellert et al., 2004). However, chlorine is not distributed uniformly across the planet. The first map of chlorine at mid-latitudes (Keller et al., 2006) revealed strong spatial variations (0.1–1%), with the Tharsis volcanic district and Meridiani region having the higher abundances.

More recently, at the Phoenix high-latitude landing site (Green Valley, 68.22°N, 125.7°W), Hecht et al. (2009) discovered perchlorate (ClO_4) (a salt of chlorine) with very high abundance (0.4–0.6%), a level found on Earth only in the Atacama desert (~0.6%, Ericksen, 1983). The existence of perchlorates in martian soil is to some extent expected (Catling et al., 2010), in view of the oxidizing and arid atmosphere of Mars and the high stability of perchlorates under Mars conditions (cold and tectonically quiescent). The origin of the perchlorates is unknown, but it is hypothesized that early volcanic activity could have produced high quantities of HCl whose chlorine was later deposited in perchlorate salts (Catling et al., 2010). Eolian saltation could grind these particles into fines that could be lofted into the high atmosphere by dust devils and dust storms where they could undergo further chemical processing, perhaps contributing a source of free elemental chlorine or its oxides.

The Viking landers detected chloromethane (CH_3Cl) during the search for organic compounds in martian soils (Biemann et al., 1976, 1977). The authors noted that CH_3Cl was evolved during pyrolysis and they assigned this signature to terrestrial contamination because it also appeared in pre-flight sampling (Biemann et al., 1976, 1977). However, the Phoenix identification of perchlorates inspired Navarro-González et al., 2010 (erratum, Navarro-González et al., 2011) to revisit this question, and to suggest instead that the Viking soil samples contained both organics and perchlorates whose pyrolytic destruction created the CH_3Cl measured. Based on kinetic modeling, Biemann and Bada (2011) challenged this view, and a lively exchange ensued (Navarro-González and McKay, 2011).

Regardless, with the abundance of chlorinated compounds established as both abundant and widespread on Mars, we now ask whether any gaseous forms of chlorine are found. The principal reservoir gas should be HCl. Krasnopolsky et al. (1997) reported an upper limit for HCl on Mars (<3 ppb, 3σ) and Hartogh et al. (2010) reported a much more sensitive limit (HCl < 0.3 ppb, 3σ), far smaller than its abundance on Venus where it is found at the ppm level (e.g., Young, 1972; Krasnopolsky, 2010) and where HCl plays a significant role in stabilizing its CO_2 atmosphere. On Venus, the very high surface temperatures permit vaporization of chlorinated salts and subsequent entry of chlorine compounds into the atmosphere. The presence of HCl or any other chlorinated species in the martian atmosphere would seemingly require currently active geological or biological sources on Mars.

Our sensitive upper limit for HCl (<0.6 ppb, 3σ) further confirms the lack of an active chlorine chemistry in the martian atmosphere, and sets contemporary limits on recent activity involving the chlorine cycle. Our upper limit for CH_3Cl (<14.3 ppb, 3σ) indicates no significant chemistry involving methyl and chlorine precursors.

4.8. Retrievals of atmospheric pressures and temperatures

In the KL infrared bands, multiple bands of carbon dioxide are observable with ground-based telescopes. The new band of isotopic carbon dioxide (628) that we recently discovered (Villanueva et al., 2008b) is among the best to probe temperatures and pressures with high-resolution ground-based spectroscopy. Under typical conditions, most of the lines of this band are optically thin, and multiple lines of different excitation energies are present over a narrow frequency range, including a strong Q-branch at 2982 cm^{-1} (3.353 μm). The fact that these lines appear in absorption is also of great value since lines at longer wavelengths (>4 μm) also show thermal emission, making retrievals more dependent on the assumed vertical profile of temperature whose uncertainty constrains the accuracy of pressure retrievals.

The first retrieval of temperatures and pressures on Mars using this new band system (Villanueva et al., 2008c; Mumma et al., 2009) provided excellent agreement with predictions of General Circulation Models (GCM, Villanueva, 2004; Millour et al., 2008). Using the same techniques, we derived pressure and column temperatures (Fig. 10) from our high-resolution CRIRES data taken on November 2009 (L_S 12°, early NH Spring). The retrieved temperatures are in very good agreement with GCM predictions, as are the pressures excepting regions of high dust and ice opacities. We cannot derive dust and ice opacities explicitly, since the breadth of their spectral features greatly exceed the limited span of our high-resolution spectra. We explored the possibility of integrating the MGS–TES scattering model (Smith, 2002) into our atmospheric model, but the high degree of uncertainty in the input parameters (dust vertical profile, dust properties, dust abundances, parameters of ice clouds, etc.) prevented us from achieving reliable results. However, our absolute retrievals of CO_2 column densities provide an indirect measure of dust and ice scattering (see Fig. 10), ultimately allowing to obtain accurate mixing ratios for all trace species at every footprint on Mars (with topographic corrections automatically included).

5. Discussion

The martian atmosphere is an arid, highly inhospitable environment – our results further confirm these conclusions. The upper layers of martian soil have been heavily eroded by long-term eolian activity, and the lack of magnetospheric and atmospheric shielding has led to modified soil chemistry (especially organics) through exposure to energetic particles. But there is ample evidence that ancient Mars was wet and likely hosted habitable conditions (e.g., Bibring et al., 2006; Carr, 1999). Moreover, the presence of extensive volcanism probably gave rise to widespread hydrothermal activity and the formation of rich subsurface aqueous reservoirs. Organics could have been produced by geological processes (e.g., serpentinization, Horita and Berndt, 1999) or even by biological activity at that time, and could have been incorporated into hydrates (Max and Clifford, 2000; Chastain and Chevrier, 2007). [Guest molecules such as methane can be trapped in "cages" of hydrogen-bonded water molecules, forming clathrate hydrates.] If such processes are now active on Mars below the permafrost, the byproduct gases could be trapped as hydrates at the base of a thickening cryosphere (Clifford and Parker, 2001).

Ground water ice has been found at depths of several centimeters by the Phoenix polar lander (Mellon et al., 2009), and massive buried glaciers were identified recently at mid-latitudes by the Mars Reconnaissance Orbiter (Holt et al., 2008). Could some such deposits contain hydrates? Hydrates containing methane can form when the required water and methane co-exist under proper thermodynamic conditions (see Fig. 4 of Chastain and Chevrier (2007)). Once formed, they are predicted to remain stable below the martian surface at even shallow depths (3–15 m), depending on the specific surface material and geothermal profile (Max and Clifford, 2000; Chastain and Chevrier, 2007; Prieto-Ballesteros et al., 2006). Hydrates can trap not only methane but also other volatiles like CO_2 (the principal gas in the Mars atmosphere), leading to more stable binary clathrates (e.g., $CH_4 + CO_2$) that could reside at even shallower depths (Sloan and Koh, 2007; Chastain and Chevrier, 2007). At the base of the cryosphere, hydrates will be stable so long as pressures in void spaces are in lithostatic equilibrium. However, should such spaces be breached to the atmosphere, the dramatic pressure drop would release pent-up gases and de-stabilize hydrates that formed since the previous breaching. We estimate that the total release observed by Mumma et al. (2009) of 42 ktons of methane (including the 19 ktons in the principal plume) would correspond to a fully-filled hydrate sphere of 88 m in diameter with at least 272 ktons of water (adopting a type I clathrate structure, Thomas et al., 2009).

While organics could be stored as hydrate in shallow and/or deep deposits, suitable mechanisms for their release are needed. There is no evidence of recent grand geological activity or major ground movement. However, one possible scenario is that rapid mass wasting or downslope movement could trigger the impulsive release of methane and water simultaneously. Repeated thermal cycling (expansion/contraction) at scarp faces in Spring/Summer could induce their defacement, shedding rocks and perhaps opening pores connecting with deep reservoirs. Gullies and debris deposits indicative of downslope movement are relatively common on Mars, and imaging from Mars Global Surveyor (Malin et al., 2006) acquired evidence of present-day gully activity near Terra Sirenum. Of course, pores in scarp faces or crater walls might open without such defacement as ice plugs sublimate upon warming during the Spring thaw.

Our data suggest that methane release is neither continuous, nor frequent. Furthermore, the lack of related VOC species (CH_3OH, H_2CO, C_2H_6, C_2H_2, C_2H_4) establishes a significant constraint on recent activity at the sites and times reported here. The non-detection of N_2O at <90 ppb is consistent with current photochemistry of N_2, and the non-detection of HCl (<0.6 ppb, in comparison to the ppm levels found on Venus) confirms that atmospheric chlorine chemistry on Mars is currently negligible, if present (see Fig. 1).

In view of the previously reported CH_4 releases (e.g., Krasnopolsky, 2012; Geminale et al., 2011; Fonti and Marzo, 2010; Mumma et al., 2009; Krasnopolsky et al., 2004; Formisano et al., 2004), our results (for CH_4 and other species) indicate a different atmospheric state, perhaps ultimately suggestive of high atmospheric variability. To fully understand the processes acting on the planet, global measurements of atmospheric composition and evolution are needed at a temporal cadence and spatial resolution consistent with the various time-varying phenomena. We have acquired the most extensive ground-based search for trace species on Mars, and our investigation reveals the need for constant global measurements of these species to clearly identify the active regions associated with the methane release observed in 2003 and to identify any other active regions on the planet.

As part of the upcoming ExoMars mission, the Trace Gas Orbiter (TGO) (Vandaele et al., 2012) would address this need. Even better would be an orbiter at the L1 Mars–Sun Lagrange point, sampling the whole illuminated disk of Mars at high spatial resolution every day (for 2 Mars years) at very high spectral resolution ($\lambda/\Delta\lambda > 10{,}000$) in the 1–5 μm region, as our team proposed in 2006 under NASA's Mars Scout Program (PI: Mumma; Bowers et al., 2006). Considering the difficulties associated with measuring organics on Mars with low-resolution instruments in Mars-orbit and from Earth using high-resolution instruments at ground-based telescopes (see Sections 4.2 and 4.3), such new sensitive searches of organics are urgently needed to further validate and expand these results.

6. Conclusions

Since 2006, we have acquired the most extensive search for trace species on Mars, now containing more than 500,000 high-resolution infrared spectra. In this paper, we presented results based on a selection of these data that sample diverse regions on the planet at different Mars seasons. We targeted multiple volatile organic species (CH_4, CH_3OH, H_2CO, C_2H_6, C_2H_2, C_2H_4), hydroperoxyl (HO_2), several nitrogen compounds (N_2O, NH_3, HCN) and two chlorine species (HCl, CH_3Cl) through their vibrational spectra in the 2.8–3.7 μm spectral region. For most of these species we derived the most stringent upper limits ever obtained, and obtained significant limits to the level of activity at several martian sites on the dates reported. Even more stringent results (or detections) might be derived once the full dataset has been evaluated.

Our non-detections of methane oxidation products (CH_3OH, H_2CO) and short-lived related species (C_2H_6, C_2H_2, C_2H_4) indicate no evidence of recent activity, while the lack of HCl establishes that atmospheric chlorine chemistry is negligible if present. Our upper limit for methane is consistent with the 2006 upper-limit reported in Mumma et al. (2009). The fact that we do not detect methane over Valles Marines in early January 2006 (just 28 days before Krasnopolsky (2012) claims a detection there) is somewhat puzzling, and seemingly requires the onset of an uniquely large release during this 28 day interval.

These metrics emphasize the need for a dedicated Mars-orbiting spacecraft with sufficient spectral resolution ($\lambda/\Delta\lambda > 10{,}000$) to properly measure the presence and evolution of trace species in the martian atmosphere, and with sufficient temporal and spatial resolution (10 km) to identify regions of active release and to establish their temporal dependence.

Acknowledgments

We thank the staff of the Very Large Telescope (VLT), the NASA InfraRed Telescope Facility (IRTF) and the W.M. Keck Observatory for their exceptional support throughout our long Mars observing Programs. G.L.V. acknowledges support from NASA's Planetary Astronomy Program (08-PAST08-0034) and NASA's Planetary Atmospheres Program (08-PATM08-0031). NASA's Planetary Astronomy Program (RTOP 344-32-07) and NASA's Astrobiology Program (RTOP 344-53-51) supported M.J.M., G.L.V and Y.L.R. NSF-RUI supported REN through Grant (AST-0805540). This work was also supported by a NASA Keck PI Data Award, administered by the NASA Exoplanet Science Institute. Data acquired at the W.M. Keck Observatory utilized telescope time allocated to the National Aeronautics and Space Administration through the agency's scientific partnership with the California Institute of Technology and the University of California. The Observatory was made possible by the generous financial support of the W.M. Keck Foundation. The authors wish to recognize and acknowledge the very significant cultural role and reverence that the summit of Mauna Kea has always had within the indigenous Hawaiian community. We are most fortunate to have the opportunity to conduct observations from this mountain.

References

Allen, M. et al., 2006. Is Mars alive? Eos 87 (4), 433–439.
Atreya, S.K., Mahaffy, P., Wong, A., 2007. Methane and related trace species on Mars: Origin, loss, implications for life, and habitability. Planet. Space Sci. 55 (3), 358–369.
Barth, C.A., Stewart, A.I.F., Bougher, S.W., Hunten, D.M., Bauer, S.J., Nagy, A.F., 1992. Aeronomy of the current martian atmosphere. In: Mars (A93-27852 09-91), pp. 1054–1089.
Bernard, B.B., Brooks, J.M., Sackett, W.M., 1976. Natural gas seepage in the Gulf of Mexico. Earth Planet. Sci. Lett. 31 (1), 48–54.
Bertaux, J.-L., Gondet, B., Lefèvre, F., Bibring, J.P., Montmessin, F., 2012. First detection of O_2 1.27 μm nightglow emission at Mars with OMEGA/MEX and comparison with general circulation model predictions. J. Geophys. Res. 117, 1–9.
Bibring, J.-P. et al., 2006. Global mineralogical and aqueous Mars history derived from OMEGA/Mars Express Data. Science 312, 400–403.
Biemann, K., Bada, J.L., 2011. Comment on "Reanalysis of the Viking results suggests perchlorate and organics at midlatitudes on Mars" by Rafael Navarro-González et al.. J. Geophys. Res. 116 (E12001), 1–5.
Biemann, K. et al., 1976. Search for organic and volatile inorganic compounds in two surface samples from the Chryse Planitia region of Mars. Science 194, 72–76.
Biemann, K. et al., 1977. The search for organic substances and inorganic volatile compounds in the surface of Mars. J. Geophys. Res. 82, 4641–4658.
Bowers, C.W. et al., 2006. The Mars organics observer: A Mars scout mission concept. Am. Astron. Soc. 38, 569.
Cardelli, J.A., Savage, B.D., Ebbets, D.C., 1990. Scattered light in the echelle modes of the Goddard high-resolution spectrograph aboard the Hubble Space Telescope. I – Analysis of prelaunch calibration data. Astrophys. J. 365, 789–802.
Carr, M.H., 1999. Retention of an atmosphere on early Mars. J. Geophys. Res. 104, 21897–21910.
Carr, M.H., Head, J.W., 2003. Oceans on Mars: An assessment of the observational evidence and possible fate . J. Geophys. Res. 108 (E5-S5042), 1–28.
Catling, D.C. et al., 2010. Atmospheric origins of perchlorate on Mars and in the Atacama. J. Geophys. Res. 115 (1), 1–15.
Chastain, B.K., Chevrier, V., 2007. Methane clathrate hydrates as a potential source for martian atmospheric methane. Planet. Space Sci. 55, 1246–1256.
Chizek, M.R., Murphy, J.R., Kahre, M.A., Haberle, R.M., Marzo, G.A., 2010. A short-lived trace gas in the martian atmosphere: A general circulation model of the likelihood of methane. Lunar Planet. Sci. 41, 1527.
Clancy, R.T., Sandor, B.J., Moriarty-Schieven, G.H., 2004. A measurement of the 362 GHz absorption line of Mars atmospheric H_2O_2. Icarus 168 (1), 116–121.
Clark, B. et al., 1976. Inorganic analyses of martian surface samples at the Viking landing sites. Science 194, 1283–1288.
Clifford, S.M., Parker, T.J., 2001. The evolution of the martian hydrosphere: Implications for the fate of a primordial ocean and the current state of the northern plains. Icarus 154, 40–79.
Clough, S.A. et al., 2005. Atmospheric radiative transfer modeling: A summary of the AER codes. J. Quant. Spectrosc. Radiat. Trans. 91, 233–244.
Davidson, J.A., Cantrell, C.A., Tyler, S.C., Shetter, R.E., Cicerone, R.J., 1987. Carbon kinetic isotope effect in the reaction of CH_4 with HO. J. Geophys. Res. 92 (D), 2195–2200.
Edwards, D.P., 1992. GENLN2: A General Line-by-Line Atmospheric Transmittance and Radiance Model. The National Center for Atmospheric Research: Technical Note 367-STR.
Encrenaz, T. et al., 1991. The atmospheric composition of Mars – ISM and ground-based observational data. Ann. Geophys. 9, 797–803, ISSN 0992-7689.
Encrenaz, T. et al., 2004a. Hydrogen peroxide on Mars: Evidence for spatial and seasonal variations. Icarus 170, 424–429.
Encrenaz, T., Lellouch, E., Atreya, S.K., Wong, A.-S., 2004b. Detectability of minor constituents in the martian atmosphere by infrared and submillimeter spectroscopy. Planet. Space Sci. 52, 1023–1037.
Encrenaz, T., Greathouse, T.K., Lefèvre, F., Atreya, S.K., 2012. Hydrogen peroxide on Mars: Observations, interpretation and future plans. Planet. Space Sci. 68 (1), 3–17.
Ericksen, G.E., 1983. The Chilean nitrate deposits. Am. Sci. 71 (4), 366–374.
Espenak, F., Mumma, M.J., Kostiuk, T., Zipoy, D., 1991. Ground-based infrared measurements of the global distribution of ozone in the atmosphere of Mars. Icarus 92, 252–262.
Fall, R., 1999. Biogenic emissions of volatile organic compounds from higher plants. React. Hydrocarbons Atmos., 41–96.
Feldman, W.C. et al., 2004. Global distribution of near-surface hydrogen on Mars. J. Geophys. Res. 109, 425–447.
Fonti, S., Marzo, G.A., 2010. Mapping the methane on Mars. Astron. Astrophys. 512 (A51), 1–5.
Formisano, V., Atreya, S.K., Encrenaz, T., Ignatiev, N., Giuranna, M., 2004. Detection of methane in the atmosphere of Mars. Science 306, 1758–1761.
Formisano, V. et al., 2005. A martian PFS average spectrum: Comparison with ISO SWS. Planet. Space Sci. 53, 1043–1052.
Gellert, R. et al., 2004. Chemistry of rocks and soils in Gusev Crater from the alpha particle X-ray spectrometer. Science 305 (5), 829–833.
Geminale, A., Formisano, V., Sindoni, G., 2011. Mapping methane in martian atmosphere with PFS-MEX data. Planet. Space Sci. 59 (2), 137–148.
Gordon, I.E. et al., 2011. HITRAN Update for C_2H_2 (Acetylene). HITRAN <http://www.cfa.harvard.edu/hitran/updates.html#Acetylene%20update>.
Greenwood, J.P., Itoh, S., Sakamoto, N., Vicenzi, E.P., Yurimoto, H., 2008. Hydrogen isotope evidence for loss of water from Mars through time. Geophys. Res. Lett. 35 (L05203), 1–5.
Hartogh, P. et al., 2010. Herschel/HIFI observations of Mars: First detection of O_2 at submillimetre wavelengths and upper limits on HCl and H_2O_2. Astron. Astrophys. 521 (L49), 1–5.
Hecht, M.H. et al., 2009. Detection of perchlorate and the soluble chemistry of martian soil at the Phoenix lander site. Science 325 (5), 64–67.
Heikes, B.G. et al., 2002. Atmospheric methanol budget and ocean implication. Global Biogeochem. Cycles 16 (4), 80–81.
Holt, J.W. et al., 2008. Radar sounding evidence for buried glaciers in the southern mid-latitudes of Mars. Science 322, 1235–1238.
Horita, J., Berndt, M.E., 1999. Abiogenic methane formation and isotopic fractionation under hydrothermal conditions. Science 285 (5430), 1055–1057.
Keller, J.M. et al., 2006. Equatorial and midlatitude distribution of chlorine measured by Mars Odyssey GRS. J. Geophys. Res. 111 (E), 1–18.
Korablev, O.I., 2002. Solar occultation measurements of the martian atmosphere on the Phobos spacecraft: Water vapor profile, aerosol parameters, and other results. Solar Syst. Res. 36 (1), 12–34.
Korablev, O.I. et al., 1993. Tentative identification of formaldehyde in the martian atmosphere. Planet. Space Sci. 41, 441–451.
Krasnopolsky, V.A., 1993. Photochemistry of the martian atmosphere (mean conditions). Icarus 101, 313–332.
Krasnopolsky, V.A., 2010. Spatially-resolved high-resolution spectroscopy of Venus 1. Variations of CO_2, CO, HF, and HCl at the cloud tops. Icarus 208 (2), 539–547.
Krasnopolsky, V.A., 2012. Search for methane and upper limits to ethane and SO_2 on Mars. Icarus 217 (1), 144–152.
Krasnopolsky, V.A., Bjoraker, G.L., 2000. Mapping of Mars $O_2(1\Delta)$ dayglow. J. Geophys. Res. 105 (E), 20179–20188.
Krasnopolsky, V.A., Bjoraker, G.L., Mumma, M.J., Jennings, D.E., 1997. High-resolution spectroscopy of Mars at 3.7 and 8 μm: A sensitive search of H_2O_2, H_2CO, HCl, and CH_4, and detection of HDO. J. Geophys. Res. 102 (E), 6525–6534.
Krasnopolsky, V.A., Maillard, J.P., Owen, T.C., 2004. Detection of methane in the martian atmosphere: evidence for life? Icarus 172, 537–547.
Kunde, V.R., Maguire, W.C., 1974. Direct integration transmittance model. J. Quant. Spectrosc. Radiat. Trans. 14, 803–817.
Lebzelter, T. et al., 2012. CRIRES-POP. A library of high resolution spectra in the near-infrared. Astron. Astrophys. 539 (A109), 1–25.
Lefèvre, F., Forget, F., 2009. Observed variations of methane on Mars unexplained by known atmospheric chemistry and physics. Nature 460 (7), 720–723.
Lefèvre, F., Lebonnois, S., Montmessin, F., Forget, F., 2004. Three-dimensional modeling of ozone on Mars. J. Geophys. Res. 109 (E07004), 1–20.
Leshin, L.A., 2000. Insights into martian water reservoirs from analyses of martian meteorite QUE94201. Geophys. Res. Lett. 27 (14), 2017–2020.
Luecken, D.J., Hutzell, W.T., Strum, M.L., Pouliot, G.A., 2012. Regional sources of atmospheric formaldehyde and acetaldehyde, and implications for atmospheric modeling. Atmos. Environ. 47, 477–490.
Maguire, W.C., 1977. Martian isotopic ratios and upper limits for possible minor constituents as derived from Mariner 9 infrared spectrometer data. Icarus 32, 85–97.
Malin, M.C., Edgett, K.S., Posiolova, L.V., McColley, S.M., Dobrea, E.Z.N., 2006. Present-day impact cratering rate and contemporary gully activity on Mars. Science 314 (5), 1573–1577.

Mancinelli, R.L., Banin, A., 2003. Where is the nitrogen on Mars? Int. J. Astrobiol. 2, 217–225.
Max, M.D., Clifford, S.M., 2000. The state, potential distribution, and biological implications of methane in the martian crust. J. Geophys. Res. 105 (E2), 4165–4171.
McElroy, M.B., Donahue, T.M., 1972. Stability of the martian atmosphere. Science 177 (4), 986–988.
McElroy, M.B., Yung, Y.L., Nier, A.O., 1976. Isotopic composition of the martian atmosphere. Science 194, 68–70.
McKay, C.P., Stoker, C.R., 1989. The early environment and its evolution on Mars: Implications for life. Rev. Geophys. 27, 189–214.
Mellon, M.T. et al., 2009. Ground ice at the Phoenix landing site: Stability state and origin. J. Geophys. Res. 114 (5), 1–15.
Millour, E. et al., 2008. The Latest (Version 4.3) Mars Climate Database. Third International Workshop on the Mars Atmosphere: Modeling and Observations, vol. 1447, p. 9029.
Mischna, M.A., Allen, M., Richardson, M.I., Newman, C.E., Toigo, A.D., 2011. Atmospheric modeling of Mars methane surface releases. Planet. Space Sci. 59 (2), 227–237.
Moyer, E.J., Irion, F.W., Yung, Y.L., Gunson, M.R., 1996. ATMOS stratospheric deuterated water and implications for troposphere–stratosphere transport. Geophys. Res. Lett. 23 (17), 2385–2388.
Mumma, M.J. et al., 2009. Strong release of methane on Mars in Northern summer 2003. Science 323 (5), 1041–1044.
Nair, H., Summers, M.E., Miller, C.E., Yung, Y.L., 2005. Isotopic fractionation of methane in the martian atmosphere. Icarus 175 (1), 32–35.
Navarro-González, R., McKay, C.P., 2011. Reply to comment by Biemann and Bada on Reanalysis of the Viking results suggests perchlorate and organics at midlatitudes on Mars. J. Geophys. Res. 116 (E12002), 1–6.
Navarro-González, R., Vargas, E., de la Rosa, J., Raga, A.C., McKay, C.P., 2010. Reanalysis of the Viking results suggests perchlorate and organics at midlatitudes on Mars. J. Geophys. Res. 115 (E12010), 1–11.
Navarro-González, R., Vargas, E., de la Rosa, J., Raga, A.C., McKay, C.P., 2011. Correction to reanalysis of the Viking results suggests perchlorate and organics at midlatitudes on Mars. J. Geophys. Res. 116 (E08011), 1–2.
Novak, R.E., Mumma, M.J., DiSanti, M.A., Dello Russo, N., Magee-Sauer, K., 2002. Mapping of ozone and water in the atmosphere of Mars near the 1997 Aphelion. Icarus 158 (1), 14–23.
Prieto-Ballesteros, O., Kargel, J.S., Fairén, A.G., Fernández-Remolar, D.C., Dohm, J.M., Amils, R., 2006. Interglacial clathrate destabilization on Mars: Possible contributing source of its atmospheric methane. Geology 34, 149–152.
Rieder, R. et al., 1997. The chemical composition of martian soil and rocks returned by the mobile Alpha Proton X-ray spectrometer: Preliminary results from the X-ray mode. Science 278, 1771–1774.
Rothman, L.S. et al., 2009. The HITRAN 2008 molecular spectroscopic database. J. Quant. Spectrosc. Radiat. Trans. 110, 533–572.
Scargle, J.D., 1982. Studies in astronomical time series analysis. II – Statistical aspects of spectral analysis of unevenly spaced data. Astrophys. J. 263, 835–853.
Siebenmorgen, R., 2007. CRIRES User Manual. User Manual, p. 97.
Sloan Jr., E.D., Koh, C., 2007. Clathrate Hydrates of Natural Gases (Chemical Industries), third ed. CRC Press.
Smith, M.D., 2002. The annual cycle of water vapor on Mars as observed by the Thermal Emission Spectrometer. J. Geophys. Res. 107 (E11-5115), 1–19.
Sowers, T., 2010. Atmospheric methane isotope records covering the Holocene period. Quatern. Sci. Rev. 29, 213–221.
Stock, J.W. et al., 2012a. Chemical pathway analysis of the martian atmosphere: CO_2-formation pathways. Icarus 219 (1), 13–24.
Stock, J.W., Grenfell, J.L., Lehmann, R., Patzer, A.B.C., Rauer, H., 2012b. Chemical pathway analysis of the lower martian atmosphere: The CO_2 stability problem. Planet. Space Sci. 68 (1), 18–24.
Sugawara, S. et al., 1997. Vertical profile of the carbon isotopic ratio of stratospheric methane over Japan. Geophys. Res. Lett. 24 (2), 2989–2992.
Thomas, C., Mousis, O., Picaud, S., Ballenegger, V., 2009. Variability of the methane trapping in martian subsurface clathrate hydrates. Planet. Space Sci. 57 (1), 42–47.
Usui, T., Alexander, C.M.O., Wang, J., Simon, J.I., Jones, J.H., 2012. Evidence from olivine-hosted melt inclusions that the martian mantle has a chondritic D/H ratio and that some young basalts have assimilated old crust. Lunar Planet. Sci. 43, 1341.
Vandaele, A.C. et al., 2012. NOMAD, a Spectrometer Suite for Nadir and Solar Occultation Observations on the ExoMars Trace Gas Orbiter. EGU General Assembly 2012 14, p. 3362.
Villanueva, G.L., 2004. The High Resolution Spectrometer for SOFIA-GREAT: Instrumentation, Atmospheric Modeling and Observations. Ph.D. Thesis, Albert-Ludwigs-Universität zu Freiburg.
Villanueva, G.L. et al., 2006. The volatile composition of the split ecliptic Comet 73P/Schwassmann–Wachmann 3: A comparison of fragments C and B. Astrophys. J. 650 (1), L87–L90.
Villanueva, G.L., Mumma, M.J., Novak, R.E., Hewagama, T., 2008a. Discovery of multiple bands of isotopic CO_2 in the prime spectral regions used when searching for CH_4 and HDO on Mars. J. Quant. Spectrosc. Radiat. Trans. 109, 883–894.
Villanueva, G.L., Mumma, M.J., Novak, R.E., Hewagama, T., 2008b. Identification of a new band system of isotopic CO_2 near 3.3 μm: Implications for remote sensing of biomarker gases on Mars. Icarus 195 (1), 34–44.
Villanueva, G.L., Mumma, M.J., Novak, R.E., Hewagama, T., Bonev, B.P., DiSanti, M.A., 2008c. Mapping the D/H of water on Mars using high-resolution spectroscopy. Mars Atmosphere: Modeling and Observations. <http://www.lpi.usra.edu/meetings/modeling2008/pdf/9101.pdf>.
Villanueva, G.L., Mumma, M.J., Magee-Sauer, K., 2011. Ethane in planetary and cometary atmospheres: Transmittance and fluorescence models of the ν7 band at 3.3 μm. J. Geophys. Res. 116 (E08012), 1–23.
Villanueva, G.L., DiSanti, M.A., Mumma, M.J., Xu, L.-H., 2012a. A quantum band model of the ν3 fundamental of methanol (CH_3OH) and its application to fluorescence spectra of comets. Astrophys. J. 747 (37), 1–11.
Villanueva, G.L., Mumma, M.J., Bonev, B.P., Novak, R.E., Barber, R.J., DiSanti, M.A., 2012b. Water in planetary and cometary atmospheres: H_2O/HDO transmittance and fluorescence models. J. Quant. Spectrosc. Radiat. Trans. 113 (3), 202–220.
Wong, A.-S., Atreya, S.K., Formisano, V., Encrenaz, T., Ignatiev, N., 2004. Atmospheric photochemistry above possible martian hot spots. Adv. Space Res. 33, 2236–2239.
Woods, T.N., Wrigley, R.T.I., Rottman, G.J., Haring, R.E., 1994. Scattered-light properties of diffraction gratings. Appl. Opt. 33 (1), 4273–4285.
Xiao, Y. et al., 2012. Methanol–CO correlations in Mexico City pollution outflow from aircraft and satellite during MILAGRO. Atmos. Chem. Phys. Discuss. 12 (2), 5705–5738.
Xu, L.-H., Wang, X., Cronin, T.J., Perry, D.S., Fraser, G.T., Pine, A.S., 1997. Sub-doppler infrared spectra and torsion-rotation energy manifold of methanol in the CH-stretch fundamental region. J. Mole. Spectrosc. 185, 158–172.
Young, L.D.G., 1972. High resolution spectra of Venus – A review. Icarus 17, 632–658.
Yung, Y.L., Demore, W.B., 1982. Photochemistry of the stratosphere of Venus – Implications for atmospheric evolution. Icarus 51, 199–247.
Zahnle, K., Freedman, R.S., Catling, D.C., 2011. Is there methane on Mars? Icarus 212 (2), 493–503.